H-p Clouds—An h-p Meshless Method

C. Armando Duarte* and J. Tinsley Oden†

TICAM — Texas Institute for Computational and Applied Mathematics, University of Texas at Austin, Taylor Hall 2.400, Austin, Texas, 78712

A new methodology to build discrete models of boundary-value problems is presented. The h-p cloud method is applicable to arbitrary domains and employs only a scattered set of nodes to build approximate solutions to BVPs. This new method uses radial basis functions of varying size of supports and with polynomial-reproducing properties of arbitrary order. The approximating properties of the h-p cloud functions are investigated in this article and a several theorems concerning these properties are presented. Moving least squares interpolants are used to build a partition of unity on the domain of interest. These functions are then used to construct, at a very low cost, trial and test functions for Galerkin approximations. The method exhibits a very high rate of convergence and has a greater ˉexibility than traditional h-p finite element methods. Several numerical experiments in 1-D and 2-D are also presented. © 1996 John Wiley & Sons, Inc.

I. INTRODUCTION

In most large-scale numerical simulations of physical phenomena, a large percentage of the overall computational effort is expended on technical details connected with meshing. These details include, in particular, grid generation, mesh adaptation to domain geometry, element or cell connectivity, grid motion and separation to model fracture, fragmentation, free surfaces, etc. Moreover, in most computer-aided design work, the generation of an appropriate mesh constitutes, by far, the costliest portion of the computer-aided analysis of products and processes.

These are among the reasons that interest in so-called meshless methods has grown rapidly in recent years. Most meshless methods require a scattered set of nodal points in the domain of interest. In these methods, there may be no fixed connectivities between the nodes, unlike the finite element or finite difference methods. This feature has significant implications in modeling some physical phenomena that are characterized by a continuous change in the geometry of the domain under analysis. The analysis of problems such as crack propagation, penetration, and large deformations, can, in principle, be greatly simplified by the use of meshless methods. A growing crack, for example, can be modeled by simply extending the free surfaces that correspond to the crack [1]. The analysis of large deformation problems by, e.g., finite element methods, may require the continuous remeshing of the domain to avoid the breakdown of the calculation due to

---

*E-mail: armando@ticam.utexas.edu.

† To whom all correspondence should be addressed; e-mail: oden@ticam.utexas.edu.

excessive mesh distortion. The use of a method that does not require successive remeshings, even after very large deformations have occurred, can dramatically simplify the modeling of this class of problems. Even in problems where only one mesh is needed for an analysis, mesh generation can be a far more time-consuming and expensive task than the construction and solution of the discrete set of equations. Therefore, a method that can deliver accurate solutions to boundary-value problems without the need of explicitly partitioning the domain could have a positive impact on many aspects of computer simulations.

Among the first methods of these types used in numerical solution of boundary-value problems are the generalized finite difference method of Liszka and Orkisz [2–4] and smoothed particle hydrodynamics (SPH) [5–8]. More recently, the importance of meshless methods is reflected by the number of new methods that have been proposed: the diffuse element method (DEM) [9], the element free Galerkin method (EFGM) [1, 10], wavelet Galerkin methods [11–13], multiquadrics [14, 15], reproducing kernel particle methods [16, 17] and the free mesh method [18].

Behind all these methods, there is an underlying approximation technique that can handle arbitrarily spaced data on complex domains; the DEM and the EFGM are based on the moving least squares method (MLSM) [19, 20]; the kernel estimates of Monaghan [7] forms the basis for the SPH method. Therefore, the first step in understanding any of these methods is the study of the underlying approximation (interpolation) technique and properties. Also, the study of the corresponding approximation technique of a meshless method can reveal its strength and weakness and reveal methods for improvement.

A comprehensive review of the meshless methods found in the literature has been prepared by Duarte [21]. The conclusion of that study is that, from the point of view of accuracy and efficiency, in spite of the variety of the meshless methods found in the literature, all the reviewed methods have serious limitations that, in most situations, can negate some of the advantages of these methods over more reliable methods such as h-p finite element methods.

The SPH method appears to be one of the most flexible of the meshless methods and is simple to implement. The SPH method uses collocation at the nodes to build a discrete set of equations governing the problem [22] and, therefore, does not require a background quadrature scheme. The price of this simplicity and flexibility is the poor accuracy of the method. A large number of nodes are usually required to achieve reasonably accuracy in practical applications. The reason for this poor accuracy is that the kernel estimation technique used in the SPH method is equivalent to the use of Shepard interpolants [21, 23], which are well known for their poor accuracy [24]. Another problem of the SPH method is the spatial instability of the method, often known as tensile instability [22].

The EFGM [1, 10] and the DEM [9] have only two major differences [1, 21]: the EFGM includes certain terms in the derivatives of the interpolants that are omitted in the DEM, and the EFGM employs Lagrange multipliers to enforce essential boundary conditions. Both methods use moving least squares functions [19] as a means of spatial discretization. These functions are used to construct a finite dimensional subspace of, e.g., $H^1(\Omega)$, and then a Galerkin method is employed to find an approximate solution in this subspace [1, 10]. Both methods have some very attractive characteristics. The MLSM can produce functions with any degree of regularity, even $C^\infty(\Omega)$, at no extra cost. Therefore, the EFGM can give, e.g., $C^1(\Omega)$ approximations of the solution of a second-order BVP. Therefore, the smoothing of fluxes used in the FEM to obtain a continuous flux may be completely unnecessary in the EFGM and DEM. These methods are applicable to arbitrary domains, and Belytschko and colleagues [1, 10, 25] have reported that the EFGM is very accurate and can achieve high rates of convergence. The method does not exhibit volumetric locking, and performance apparently is only minimally affected by irregular placement of nodes. The main drawbacks of the method are the cost of building the moving

least squares functions and the need of a background quadrature scheme to evaluate the integrals that appear in the weak forms used by the Galerkin method. Another difficulty appears in the construction of the MLS functions. There must be an increase in the size of the support of these functions, if one wants to increase the polynomial degree that the MLS functions can represent through linear combinations. Also, there are some nodal arrangements that can break down the algorithm used to construct the MLS functions [21].

Another limitation of the meshless methods found in the literature is that none of them, except the wavelet method in one dimension [12] and the generalized finite difference method, has a rich mathematical background to justify their use. That is, mathematical proofs of conditions sufficient to guarantee that these methods will converge to the true solution are not available.

This article presents a new family of meshless methods for the solution of boundary-value problems. The *h-p* cloud method is applicable to arbitrary domains and employs only a scattered set of nodes to build approximate solutions to boundary-value problems. The method uses radial basis functions of varying size of supports and with polynomial reproducing properties of arbitrary order. The first numerical experiments with this technique show very promising results.

The next sections of this article describe in detail the *h-p* cloud method. Following this introduction, Section II introduces the *h-p* cloud family of spaces $\mathcal{F}_N^{k,p}$. *a-priori* error estimates for the *h* version of the method are presented in Section III. Finally, Sections IV and V present the results of numerical experiments involving approximation of functions by *h-p* clouds and solutions of boundary-value problems in one and two dimensions.

II. *H-P* CLOUDS: HIGH-ORDER APPROXIMATION OF SCATTERED DATA

A. Introduction

In this section, a technique for approximating functions defined on an open bounded domain $\Omega \in \mathbb{R}^n, n = 1, 2$, or 3 is presented. The method employs only an arbitrarily scattered set of nodes belonging to Ω.

B. Partition of Unity

One fundamental idea used in the construction of the *h-p* cloud spaces is that of a partition of unity. In this section, the construction of the partition of unity used in the *h-p* cloud method is described. Some properties of these functions are also investigated. We begin by introducing some notation used throughout the article.

We assume that Ω is an open bounded domain in $\mathbb{R}^n, n = 1, 2$, or 3. Q_N denotes an arbitrarily chosen set of N nodes $x_\alpha \in \Omega$.

$$Q_N = \{x_1, x_2, \ldots, x_N\}, x_\alpha \in \Omega.$$

The set Q_N is used to define a finite open covering $T_N := \{\omega_\alpha\}_{\alpha=1}^N$ of Ω composed of N balls ω_α centered at the points $x_\alpha, \alpha = 1, \ldots, N$, where

$$\omega_\alpha := \{y \in \mathbb{R}^n : \|x_\alpha - y\|_{\mathbb{R}^n} < h_\alpha\}$$

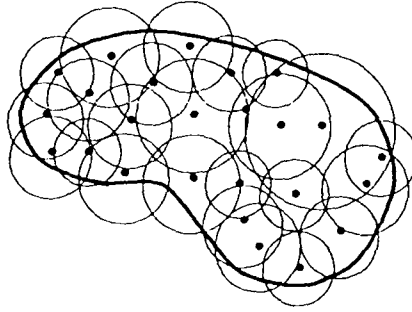$$\bar{\Omega} \subset \bigcup_{\alpha=1}^N \omega_\alpha.$$

FIG. 1.   Open covering in 2-D with balls centered at the nodes.

A class of functions $\{\varphi_\alpha\}_{\alpha=1}^N$ is called a partition of unity subordinate to the open covering $\mathcal{T}_N$, if it possesses the following properties:

1) $\qquad \varphi_\alpha \in C_0^\infty(\omega_\alpha), \qquad 1 \le \alpha \le N$

2) $\qquad \displaystyle\sum_{\alpha=1}^N \varphi_\alpha(x) = 1, \qquad \forall x \in \Omega.$

Construction of a Partition of Unity

There is no unique way to build a partition of unity as defined above. In the h-p cloud method we use the following approach:

Let $\mathcal{W}_\alpha : \mathbb{R}^n \to \mathbb{R}$ denote a weighting function that belongs to the space $C_0^s(\omega_\alpha), s \ge 0$, with the following properties:

$$\mathcal{W}_\alpha(y) \ge 0 \qquad \forall y \in \Omega$$

$$\mathcal{W}_\alpha(y) := W_\alpha(y - x_\alpha),$$

where the functions $W_\alpha \in C_0^s(\mathcal{B}_{h_\alpha}), s \ge 0$, and are defined over a ball $\mathcal{B}_{h_\alpha}$ of radius h_α centered at the origin

$$\mathcal{B}_{h_\alpha} = \{x \in \mathbb{R}^n : \|x\|_{\mathbb{R}^n} < h_\alpha\}.$$

Next, we introduce a family of functionals defined over continuous functions defined on Ω by

$$(f, g)_y := \sum_{\alpha=1}^N \mathcal{W}_\alpha(y)f(x_\alpha)g(x_\alpha), \qquad f, g : \Omega \to \mathbb{R}, f, g \in C^l(\Omega), l \ge 0. \qquad (2.1)$$

Assumption 2.1.   Given a set of m functions $\mathbb{P} = \{P_1, P_2, \ldots, P_m\}, P_i : \Omega \to \mathbb{R}, P_i \in C^l(\Omega), l \ge 0$ for $i = 1, \ldots, m$, the weighting functions $\mathcal{W}_\alpha$ defined above and the functions P_i are such that $\forall x \in \bar{\Omega}$ there holds

$$\sum_{k=1}^m a_k(P_k, P_l)_x \equiv 0 \text{ for } l = 1, \ldots, m \text{ if and only if } a_k \equiv 0 \text{ for } k = 1, \ldots, m.$$

The following result is due to Ainsworth [26].

Proposition 2.1.   *If the Assumption 2.1 holds, then the functional $(.,.)_x$ defined in (2.1) is an inner product on $\mathrm{span}(\mathbb{P})$.*

Proof.   The proof involves only standard algebraic manipulations. Details can be found in [27].   ∎

The next theorem gives us necessary, and in some cases sufficient, conditions for the satisfaction of Assumption 2.1.

Theorem 2.1.   *A necessary condition for the satisfaction of the Assumption 2.1 is that for any* $y, \in \Omega$ *there exist indices* $\alpha_1, \ldots, \alpha_k, k \geq \#\mathbb{P} = m$, *dependent on* y, *such that*

$$y \in \bigcap_{j=1}^{k} supp(\mathcal{W}_{\alpha_j}). \tag{2.2}$$

If $\#\mathbb{P} = 1$, *then the above condition is also sufficient. If* $\bar{\Omega} \subset \mathbb{R}^2$ *and* $\mathbb{P} = \{1, x, y\}$ *and in addition to the above condition* $x_{\alpha_1}, \ldots, x_{\alpha_k}$ *contains a subset of 3 points not aligned, then the above condition is also sufficient.*

Proof.   Let y be an arbitrary point in $\bar{\Omega}$ and suppose that the indices $\alpha_1, \ldots, \alpha_k$ are such that (2.2) is true. Then the matrix $A(y) := (P_i, P_j)_y$ can be written as

$$
\begin{bmatrix}
P_1(x_{\alpha_1}) & P_1(x_{\alpha_2}) & \cdots & P_1(x_{\alpha_k}) \\
P_2(x_{\alpha_1}) & P_2(x_{\alpha_2}) & \cdots & P_2(x_{\alpha_k}) \\
\vdots & \vdots & \ddots & \vdots \\
P_m(x_{\alpha_1}) & P_m(x_{\alpha_2}) & \cdots & P_m(x_{\alpha_k})
\end{bmatrix}
*
\begin{bmatrix}
\mathcal{W}_{\alpha_1}(y) & 0 & \cdots & 0 \\
0 & \mathcal{W}_{\alpha_2}(y) & \cdots & 0 \\
\vdots & \vdots & \ddots & \vdots \\
0 & 0 & \cdots & \mathcal{W}_{\alpha_k}(y)
\end{bmatrix}
*
$$

$$
*
\begin{bmatrix}
P_1(x_{\alpha_1}) & P_2(x_{\alpha_1}) & \cdots & P_m(x_{\alpha_1}) \\
P_1(x_{\alpha_2}) & P_2(x_{\alpha_2}) & \cdots & P_m(x_{\alpha_2}) \\
\vdots & \vdots & \ddots & \vdots \\
P_1(x_{\alpha_k}) & P_2(x_{\alpha_k}) & \cdots & P_m(x_{\alpha_k})
\end{bmatrix}
:= FWF^T.
$$

The rank of F, and consequently of A, will be at most equal to k, so, for A to be positive definite, we must have $k \geq m$.

Now suppose that $\#\mathbb{P} = 1$ and, without loss of generality, that $P_1 = 1$. In this case, the matrix $(P_k, P_l)_y$ reduces to a single entry

$$A(y) = \sum_{j=1}^{k} \mathcal{W}_{\alpha_j}(y),$$

which is a positive number from the definition of the weighting functions and from (2.2). Therefore, in this case, the conditions of the theorem are also sufficient.

Let $\bar{\Omega} \subset \mathbb{R}^2, \mathbb{P} = \{1, x, y\}$, and $x_{\alpha_a}, x_{\alpha_b}, x_{\alpha_c}$ be the three points not aligned. In this case, the matrix F defined before reduces to

$$
F =
\begin{bmatrix}
1 & 1 & \cdots & 1 \\
x_{\alpha_a} & x_{\alpha_b} & \cdots & x_{\alpha_c} \\
y_{\alpha_a} & y_{\alpha_b} & \cdots & y_{\alpha_c}
\end{bmatrix}.
$$

The rows of F are linearly independent, since

$$
\begin{vmatrix}
1 & 1 & 1 \\
x_{\alpha_a} & x_{\alpha_b} & x_{\alpha_c} \\
y_{\alpha_a} & y_{\alpha_b} & y_{\alpha_c}
\end{vmatrix}
= 2 * \Delta,
$$

where Δ is the area of a triangle having the nodes $x_{\alpha_a}, x_{\alpha_b}, x_{\alpha_c}$ as vertices. Thus, the $rank(\boldsymbol{F}) = 3$ and $rank(\boldsymbol{F}^T) = 3$. Also $\boldsymbol{W}$ is positive definite since $\mathcal{W}_{\alpha_j}(y) > 0, j = 1, \ldots, k$. These imply that $\boldsymbol{A}$ is positive-definite. ∎

We are now in a position to define the partition of unity used in the h-p cloud method. The partition of unity function φ_α associated with the ball ω_α is defined by

$$\varphi_\alpha(x) := \mathbb{P}^T(x)\boldsymbol{A}^{-1}(x)B_\alpha(x), \tag{2.3}$$

where:

- $\mathbb{P}(x) := \{P_1(x), P_2(x), \ldots, P_m(x)\}^T, \exists P_j \; s.t. \; P_j(x) \equiv 1$
- $A_{ij}(x) := (P_i, P_j)_x,$
- $B_\alpha(x) := \mathcal{W}_\alpha(x)\mathbb{P}(x_\alpha).$

Theorem 2.2. *If $P_i, i = 1, \ldots, m, \in C^l(\Omega), l \geq 0,$ and $\mathcal{W}_\alpha, \alpha = 1, \ldots, N, \in C^q(\Omega), q \geq 0,$ then $\varphi_\alpha(x)$ as defined above $\in C^{\min(l,q)}(\Omega)$.*
   Proof.   Define

$$C_\alpha(x) := \boldsymbol{A}^{-1}(x)B_\alpha(x),$$

then

$$\varphi_\alpha(x) = \mathbb{P}^T(x)C_\alpha(x)$$

and

$$\boldsymbol{A}(x)C_\alpha(x) = B_\alpha(x).$$

Thus, using the Leibniz formula [28],

$$D^\beta(\boldsymbol{A}C_\alpha) = \sum_{\gamma \leq \beta} \binom{\beta}{\gamma} D^\gamma \boldsymbol{A} D^{\beta-\gamma} C_\alpha = D^\beta B_\alpha$$

$$= \boldsymbol{A}D^\beta C_\alpha + \sum_{\substack{\gamma \leq \beta \\ \gamma \neq 0}} \binom{\beta}{\gamma} D^\gamma \boldsymbol{A} D^{\beta-\gamma} C_\alpha$$

$$D^\beta C_\alpha = \boldsymbol{A}^{-1}\left[D^\beta B_\alpha - \sum_{\substack{\gamma \leq \beta \\ \gamma \neq 0}} \binom{\beta}{\gamma} D^\gamma \boldsymbol{A} D^{\beta-\gamma} C_\alpha \right].$$

The last expression makes sense, since by Assumption 2.1 $\boldsymbol{A}^{-1}$ exists, and by the assumptions on the differentiability of $\mathcal{W}_\alpha$ and $P_i, D^\beta B_\alpha$ and $D^\beta \boldsymbol{A}$ also exists, if $|\beta| \leq \min(l, q)$. The lower-order derivatives of C_α that appear on the right-hand side can be computed recursively using the above expression. So, we conclude that $C_\alpha \in C^{\min(l,q)}(\Omega)$, and the conclusion of the theorem is immediate. ∎

Theorem 2.3. *The partition of unity functions φ_α are $\mathbb{P}$-reducible for the set Q_N; that is, given any element $P_j \in \mathbb{P}$, the following holds $\forall x \in \bar{\Omega}$:*

$$P_j(x) = \sum_{\alpha=1}^{N} P_j(x_\alpha)\varphi_\alpha(x). \qquad (2.4)$$

If the constant $1 \in \mathbb{P}$, then

$$\sum_{\alpha=1}^{N} \varphi_\alpha(x) = 1 \qquad \forall x \in \bar{\Omega}.$$

Proof. Let $P_l \in \mathbb{P}$. From the definition of φ_α given in (2.3),

$$
\begin{aligned}
\sum_{\alpha=1}^{N} P_l(x_\alpha)\varphi_\alpha(x) &= \sum_{\alpha=1}^{N} P_l(x_\alpha) \sum_{j,k=1}^{m} P_k(x) A_{kj}^{-1}(x) W_\alpha(x) P_j(x_\alpha) \\
&= \sum_{j,k=1}^{m} \sum_{\alpha=1}^{N} P_l(x_\alpha) P_j(x_\alpha) W_\alpha(x) A_{kj}^{-1}(x) P_k(x) \\
&= \sum_{j,k=1}^{m} A_{lj}(x) A_{jk}^{-1}(x) P_k(x) = P_l(x),
\end{aligned}
$$

which shows that the functions φ_α are $\mathbb{P}$-reducible for the set Q_N.

Since $1 \in \mathbb{P}$, the above gives

$$1 = \sum_{\alpha=1}^{N} 1(x_\alpha)\varphi_\alpha(x) = \sum_{\alpha=1}^{N} \varphi_\alpha(x).$$

∎

The set of functions $\mathbb{P}$ is, in general, a set of complete polynomials in $\mathbb{R}^n$ and, therefore, they are $C^\infty(\Omega)$ functions. The weighting functions W_α can be constructed in such a way that they are also $C^\infty(\Omega)$ functions [21]. Therefore, the two previous theorems show that if the functions P_i and the weighting functions W_α are sufficiently smooth, the definition of φ_α given in (2.3) satisfies the definition of a partition of unity and, in addition, they are $\mathbb{P}$-reducible for the set Q_N.

Remark. The partition of unity functions defined in (2.3) are known as moving least squares functions (MLSF) [19] and they can also be built using a constructive approach [27].

C. The Families $\mathcal{F}_N^{k,p}$

The most important step in the h-p cloud method is the construction of the family of functions $\mathcal{F}_N^{k,p}$ using a partition of unity $\{\varphi_\alpha\}_{\alpha=1}^{N}$ as the one defined in the previous section. This class of functions can be constructed at a very low cost and has the important property that $\mathcal{P}_p \subset span\{\mathcal{F}_N^{k,p}\}$, where $\mathcal{P}_p$ denotes the space of polynomials of degree less or equal p. In this section, we describe the construction of $\mathcal{F}_N^{k,p}$ and prove some theorems concerning fundamental properties of these functions.

Let $\mathcal{L}_p$ denote a set of tensor product complete polynomials L_{ijm} in $\mathbb{R}^3$:

$$L_{ijm} = L_i(x_1)L_j(x_2)L_m(x_3), \qquad 0 \le i,j,m \le p.$$

Other sets of complete polynomials can be used as well, e.g., the smallest set of complete polynomials Π_p. In the following, the set $S_N^k := \{\varphi_\alpha^k\}_{\alpha=1}^{N}$ denotes a partition of unity that is $\mathcal{L}_k$-reducible

for the set Q_N, that is, given any element $L_{ijm} \in \mathcal{L}_k$, the following holds $\forall x \in \bar{\Omega}$:

$$L_{ijm}(x) = \sum_{\alpha=1}^{N} L_{ijm}(x_\alpha)\varphi_\alpha^k(x).$$

The family of functions $\mathcal{F}_N^{k,p}$ is defined by

$$\mathcal{F}_N^{k,p} = \{\{\varphi_\alpha^k(x)\} \cup \{\varphi_\alpha^k L_{ijm}(x)\} : 1 \leq \alpha \leq N; 0 \leq i,j,m \leq p, i \text{ or } j \text{ or } m > k; p \geq k\}.$$

(2.5)

The idea behind the definition in (2.5) is to add, hierarchically, appropriate elements to the set $\mathcal{S}_N^k$ such that the resulting set can represent, through linear combinations, polynomials of degree $p \geq k$. Because of property 2) of a partition of unity, those elements are precisely the product of the functions φ_α^k with the elements from the set $\mathcal{L}_p$ that are missing from the set $\mathcal{L}_k$. Figures 2 and 3 illustrate the situation for the case $n = 2, k = 1$, and $p = 3$, when $\mathcal{L}_p$ and $\mathcal{L}_k$ are sets of tensor product polynomials in $\mathbb{R}^2$, and when $\mathcal{L}_p$ and $\mathcal{L}_k$ are equal to $\Pi_p(\mathbb{R}^2)$ and $\Pi_k(\mathbb{R}^2)$, respectively.

For consistent results, regardless of the scale of the problem, the h-p cloud functions introduced in (2.5) are implemented using maps given by

$$F_\alpha : \hat{\omega}_\alpha \to \omega_\alpha$$

$$F_\alpha(\xi) = h_\alpha \xi + x_\alpha, \qquad \xi \in \hat{\omega}_\alpha,$$

where

$$\hat{\omega}_\alpha := \{\xi \in \mathbb{R}^n : \|\xi\|_{\mathbb{R}^n} < 1\}$$

is a sphere/circle/segment of radius one, and

$$\omega_\alpha := \{x \in \mathbb{R}^n : \|x_\alpha - x\|_{\mathbb{R}^n} < h_\alpha\}$$

is the support of the function φ_α.

The h-p cloud function $\varphi_\alpha L_{ijm}(x)$ is implemented in $\mathbb{R}^3$ by

$$\varphi_\alpha L_{ijm}(x) := \varphi_\alpha(x)(\hat{L}_{ijm} \circ F_\alpha^{-1}(x)),$$

where $\hat{L}_{ijm}(\xi)$ is a tensor product polynomial defined on $[-1,1]^3$.

		$L_0(x_2)$	$L_1(x_2)$	$L_2(x_2)$	$L_3(x_2)$	...
	$L_0(x_1)$	$L_0 L_0$	$L_0 L_1$	$\underline{L_0 L_2}$	$\underline{L_0 L_3}$	...
$k = 1$	$L_1(x_1)$	$L_1 L_0$	$L_1 L_1$	$\underline{L_1 L_2}$	$\underline{L_1 L_3}$	...
	$L_2(x_1)$	$\underline{L_2 L_0}$	$\underline{L_2 L_1}$	$\underline{L_2 L_2}$	$\underline{L_2 L_3}$	...
$p = 3$	$L_3(x_1)$	$\underline{L_3 L_0}$	$\underline{L_3 L_1}$	$\underline{L_3 L_2}$	$\underline{L_3 L_3}$	...
	$\vdots$	$\vdots$	$\vdots$	$\vdots$	$\vdots$	$\ddots$

FIG. 2.   The elements L_{ij} used to build the family $\mathcal{F}_N^{k=1, p=3}$, when tensor product polynomials are used, are those underlined.

$$L_0 L_0$$

$$k = 1 \qquad L_1 L_0 \quad L_0 L_1$$

$$\underline{L_2 L_0} \quad \underline{L_1 L_1} \quad \underline{L_0 L_2}$$

$$p = 3 \quad \underline{L_3 L_0} \quad \underline{L_2 L_1} \quad \underline{L_1 L_2} \quad \underline{L_0 L_3}$$

$$\vdots$$

FIG. 3. The elements L_{ij} used to build the family $\mathcal{F}_N^{k=1,p=3}$, when the sets $\Pi_{k=1}(\mathbb{R}^2)$ and $\Pi_{p=3}(\mathbb{R}^2)$ are used, are those underlined.

The family $\mathcal{F}_N^{k,p}$ represents a generalization of some classes of functions used in diverse fields such as interpolation of functions [19, 29] and solution of boundary-value problems [3]. The Shepard functions [29] corresponds to the family

$$\mathcal{F}_N^{k=0,p=0} = \{\varphi_1^0, \varphi_2^0, \ldots, \varphi_N^0\}.$$

The approximation technique developed by Liszka (with the appropriate choice of the stars, see [3] for more details) [2, 3] corresponds to the family

$$\mathcal{F}_N^{k=2,p=2} = \{\varphi_1^2, \varphi_2^2, \ldots, \varphi_N^2\}.$$

The moving least squares method developed by [19] and used in the element free Galerkin method [1, 10] corresponds to the use of the families

$$\mathcal{F}_N^{k,p=k} = \{\varphi_1^k, \varphi_2^k, \ldots, \varphi_N^k\}.$$

The class of functions used in the h-p cloud method is a generalization of the above:

$$\mathcal{F}_N^{k,p} = \left\{ \begin{array}{cccc} \varphi_1^k, & \varphi_2^k, & \cdots, & \varphi_N^k \\ \varphi_1^k L_{s=1}, & \varphi_2^k L_{s=1}, & \cdots, & \varphi_N^k L_{s=1}, \\ \varphi_1^k L_{s=2}, & \varphi_2^k L_{s=2}, & \cdots, & \varphi_N^k L_{s=2}, \\ \vdots & \vdots & \ddots & \vdots \\ \varphi_1^k L_{s=M}, & \varphi_2^k L_{s=M}, & \cdots, & \varphi_N^k L_{s=M} \end{array} \right\},$$

where M depends on the set of polynomials used. If tensor product polynomials are used in $\mathbb{R}^n$, then

$$M = ((p+1)^n - (k+1)^n).$$

Theorem 2.4. *The set $\mathcal{F}_N^{k,p}$ has the following properties:*

i) *If the partition of unity functions $\{\varphi_\alpha^k\}_{\alpha=1}^N$ are linearly independent in $\mathbb{R}^n$, then the set $\mathcal{F}_N^{k,p}$ is also a linearly independent set of functions in $\mathbb{R}^n$.*

ii) *dim $\mathcal{F}_N^{k,p} = N + N((p+1)^n - (k+1)^n)$, if tensor product polynomials are used in $\mathbb{R}^n$.*

iii) *dim $\mathcal{F}_N^{k,p} = N + N(\binom{p+n}{p} - \binom{k+n}{k})$, if the sets $\prod_k(\mathbb{R}^n)$ and $\prod_p(\mathbb{R}^n)$ of complete polynomials are used in $\mathbb{R}^n$.*

Proof. (for $n = 3$) Suppose that

$$\sum_\alpha^N \left(a_\alpha \varphi_\alpha^k(x) + \sum_{\substack{0 \le i,j,m \le p \\ i \text{ or } j \text{ or } m > k}} b_{\alpha ijm} \varphi_\alpha^k L_{ijm}(x) \right) = 0$$

$$\sum_{\alpha}^{N} \varphi_{\alpha}^{k}(x) \left(a_{\alpha} + \sum_{\substack{0 \leq i,j,m \leq p \\ i \text{ or } j \text{ or } m > k}} b_{\alpha ijm} L_{ijm}(x) \right) = 0.$$

Since $\{\varphi_{\alpha}^{k}\}_{\alpha=1}^{N}$ is a linearly independent set, we must have

$$a_{\alpha} + \sum_{\substack{0 \leq i,j,m \leq p \\ i \text{ or } j \text{ or } m > k}} b_{\alpha ijm} L_{ijm}(x) = 0 \qquad \alpha = 1, \ldots, N.$$

Since the set $\{L_{ijm}\}$ is a linearly independent set and there is no linear combination of the functions $L_{ijm}(x)$ that is equal to a constant, we must have

$$a_{\alpha} \equiv 0, \qquad b_{\alpha ijm} \equiv 0.$$

The proofs of (ii) and (iii) follow directly from the definition (2.5). ∎

Theorem 2.5. $\mathcal{L}_{p} \subset span\{\mathcal{F}_{N}^{k,p}\}$.

Proof. If $L_{rst}, 0 \leq r,s,t \leq p \in span\{\mathcal{F}_{N}^{k,p}\}$, then $\exists a_{\alpha}$ and $b_{\alpha ijm}$ such that

$$L_{rst}(x) = \sum_{\alpha}^{N} \left(a_{\alpha} \varphi_{\alpha}^{k}(x) + \sum_{\substack{0 \leq i,j,m \leq p \\ i \text{ or } j \text{ or } m > k}} b_{\alpha ijm} \varphi_{\alpha}^{k} L_{ijm}(x) \right).$$

If r, s, and $t \leq k$, then

$$a_{\alpha} = L_{rst}(x_{\alpha}) \qquad \alpha = 1, \ldots, N$$

$$b_{\alpha ijm} \equiv 0$$

will work, since the functions φ_{α}^{k} are $\mathcal{L}_{k}$-reducible.

If r or s or $t > k$, then take

$$a_{\alpha} \equiv 0$$

$$b_{\alpha ijm} = \begin{cases} 1 & \text{if } i = r, j = s, m = t \\ 0 & \text{otherwise} \end{cases} \qquad \alpha = 1, \ldots, N,$$

then

$$\sum_{\alpha}^{N} \left(a_{\alpha} \varphi_{\alpha}^{k}(x) + \sum_{\substack{0 \leq i,j,m \leq p \\ i \text{ or } j \text{ or } m > k}} b_{\alpha ijm} \varphi_{\alpha}^{k} L_{ijm}(x) \right)$$

$$= \sum_{\alpha}^{N} (b_{\alpha rst} \varphi_{\alpha}^{k} L_{rst}(x)) = L_{rst}(x) \sum_{\alpha}^{N} \varphi_{\alpha}^{k}(x) = L_{rst}(x). \quad ∎$$

Plot of the h-p Cloud Shape Functions

The definition of the partition of unity functions give in (2.3) shows that, except for special cases, there is no closed form for these functions. The same applies for the cloud functions from the families $\mathcal{F}_{N}^{k,p}$ defined in (2.5). In this section, h-p cloud functions corresponding to various choices of k and p are plotted in 2-D.

The following weighting function is used to build the partition of unity:

$$
\mathcal{W}_\alpha(\|y - x_\alpha\|_{\mathbb{R}^2}) = \left\{
\begin{array}{ll}
\sqrt{4/\pi} \left(1.0 - \frac{\|y - x_\alpha\|_{\mathbb{R}^2}^2}{h_\alpha^2}\right)^4 & \text{if } \|y - x_\alpha\|_{\mathbb{R}^2} < h_\alpha \\
0 & \text{if } \|y - x_\alpha\|_{\mathbb{R}^2} \geq h_\alpha
\end{array}
\right. ,
$$

where h_α is the radius of the circle ω_α.

Figure 4 shows the node arrangement and the associated covering $\mathcal{T}_{N=25}$ used to build the partition of unity functions φ_α^k. The domain Ω is either the square $(-1, 1) \times (-1, 1)$ or the square $(0, 1) \times (0, 1)$. The set $\mathbb{P}$, used to build the functions φ_α^k, is composed of tensor product of one-dimensional polynomials of degree less or equal to k. The families $\mathcal{F}_N^{k,p}$ are also built using tensor product polynomials as defined in (2.5).

The following algorithm is used to automatically set the size h_α of the support of the functions. The algorithm guarantees that Assumption 2.1 is satisfied when k is equal to 0 or 1. If $k \geq 2$, the algorithm guarantees that the necessary conditions for the satisfaction of Assumption 2.1 are met. In next sections, we show that in the h-p cloud method there is no advantage in using $k > 0$, which justifies the use of the algorithm in practical computations. The algorithm is described for the two-dimensional case. The extension to the three-dimensional case is straightforward. A similar algorithm has recently been proposed by [30] in the context of the element-free Galerkin method.

Let Q denote the index set of all points in Ω that we want to build a cloud function using partition of unity functions φ^k.

For all balls ω_α set $h_\alpha = 0$.

For all points $\xi_k \in Q$ do:

○ *Build a list List of all nodes that fall within a searching square centered at ξ_k and with sides equal to $2 * R$, where $R =$ upper bound for h_α. If $\dim(List) < \dim(\mathbb{P})$ increase the size of the searching square and try again.*

○ *Build a list Dist with the distance from the nodes in List to the point ξ_k.*

○ *Sort the list Dist.*

○ *Enforce that ξ_k belongs to the support of the $\dim(\mathbb{P})$ closest nodes in List. This is accomplished using the list Dist and the values of h_α.*

○ *If $k = 1$, check if there are at least 3 nodes in the list of the $\dim(\mathbb{P})$ closest nodes that are not aligned. If necessary, enforce that ξ_k belongs also to the support of other nodes in the list List.*
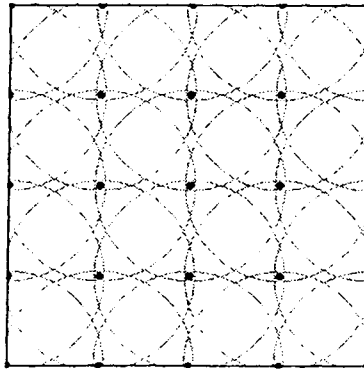

FIG. 4. Node arrangement and support of functions.

End do.

Multiply the radius h_α of the balls ω_α by a factor $\beta = 1.5$.

The above algorithm requires an efficient means of determining which nodes fall within a specified region of the domain. This same kind of problem appears in the smoothed particle hydrodynamics method [22]. Swegle and colleagues [22] developed a very efficient algorithm to perform this kind of search. The algorithm can be used in any dimension, and the total execution time of the algorithm is of order $\dim(Q)\log(N)$, where N is the total number of nodes. This algorithm is used in our implementation.

Figure 5(a) shows the function $\varphi_{\alpha=13}^{k=1}$ associated with node $x_{13} = (0,0)$. This function belongs to the families $\mathcal{F}_{N=25}^{k=1,p\geq1}$. The product of the function $\varphi_{\alpha=13}^{k=1}$ with y^2 is shown in Fig. 5(b). This corresponds to the h-p cloud function $y^2\varphi_{\alpha=13}^{k=1}$, which belongs to the families $\mathcal{F}_{N=25}^{k=1,p\geq2}$. Figure 5(c) shows the h-p cloud function $xy^2\varphi_{\alpha=13}^{k=1}$, which was built by multiplying the function shown in Fig. 5(a) by xy^2. This function belongs to the families $\mathcal{F}_{N=25}^{k=1,p\geq3}$. The partition of unity function $\varphi_{\alpha=1}^{k=2}$ associated with node $x_1 = (-1,-1)$ is depicted in Fig. 5(d). Note that the function is not defined outside of Ω. This function belongs to the families $\mathcal{F}_{N=25}^{k=2,p\geq2}$.

III. APPROXIMATION THEORY FOR THE H-P CLOUD METHOD-H CONVERGENCE

A. Introduction

In this section, we consider the problem of determining estimates in appropriate norms and seminorms of the difference $(u - u_h)$, where u is a function that belongs to a given Sobolev space X and u_{hp} is an approximation of u built using h-p cloud methods and belonging to a subspace X^{hp} of X.

The strategy used to derive the local estimates follows closely that of [31, 32] in the context of finite element methods. The approach used to derive the global estimates follows [33, 34].

B. Preliminaries

We define a ball in $\mathbb{R}^n$ as the triple $(\bar{\omega}_\alpha, \Xi_\alpha^{hp}, \mathbb{L}_\alpha^2)$, where:

(i) $\bar{\omega}_\alpha$ is a closed subset of $\mathbb{R}^n$ given by

$$\bar{\omega}_\alpha := \overline{\{y \in \mathbb{R}^n : \|x_\alpha - y\|_{\mathbb{R}^n} < h_\alpha\}} \qquad x_\alpha \in \bar{\Omega}.$$

(ii) Ξ_α^{hp} is a space of real-valued functions defined over the set $\bar{\omega}_\alpha$ and given by

$$\Xi_\alpha^{hp} := \operatorname{span}\{\mathcal{F}_N^{k,p}|_{\omega_\alpha}\} \equiv \operatorname{span}\{\Phi_j^\alpha\}_{j\in I},$$

where $\mathcal{F}_N^{k,p}$ is the set of global cloud functions defined in previous section, $\Phi_j^\alpha \in$ basis of Ξ_α^{hp}, that is, it is a shape function, and I is an index set.

(iii) $\mathbb{L}_\alpha^2$ is a set of linearly independent linear forms a_l, where $l \in I$, defined over the space Ξ_α^{hp} and given by

$$a_l(v) := \sum_{j\in I}(M_{lj}^\alpha)^{-1}(v, \Phi_j^\alpha)_{L^2(\omega_\alpha)}, \tag{3.1}$$

where

- $v \in \Xi_\alpha^{hp}$

(a) 2-D function: $\varphi_{\alpha=13}^{k=1}$

(b) 2-D function: $y^2 \varphi_{\alpha=13}^{k=1}$

(c) 2-D function: $xy^2 \varphi_{\alpha=13}^{k=1}$
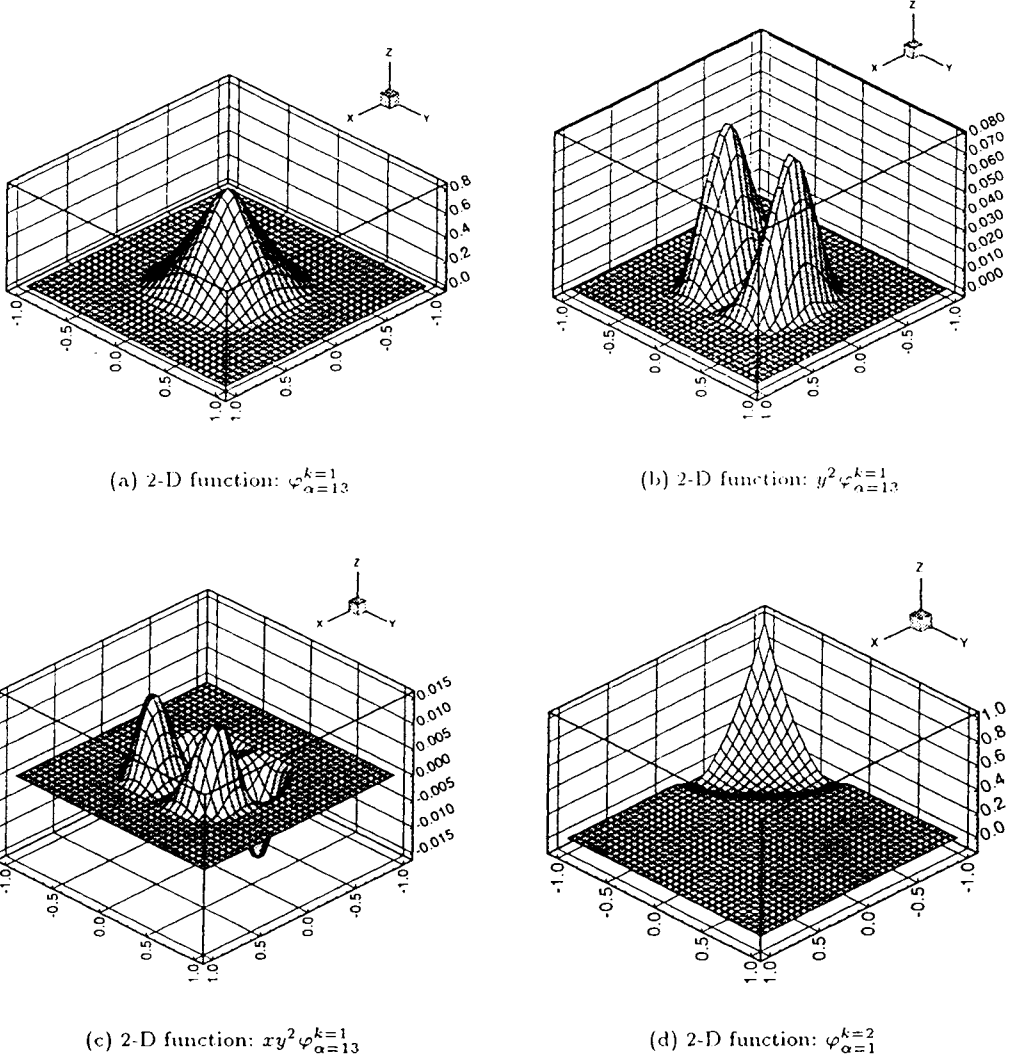

(d) 2-D function: $\varphi_{\alpha=1}^{k=2}$

FIG. 5.   Plot of 2-D *h-p* cloud functions.

- $M_{lj}^{\alpha} = (\Phi_l^{\alpha}, \Phi_j^{\alpha})_{L^2(\omega_\alpha)} = \int_{\omega_\alpha} \Phi_l^{\alpha} \Phi_j^{\alpha} \, dx.$

The functionals a_l are denoted by degrees of freedom.

Given a ball $(\bar{\omega}_\alpha, \Xi_\alpha^{hp}, \mathbb{L}_\alpha^2)$, and given a function $v : \bar{\omega}_\alpha \to \mathbb{R}$ sufficiently smooth so that the degrees of freedom $a_l, l \in I$, are well defined, we let

$$\Pi_\alpha^2 v := \sum_{i \in I} a_i(v) \Phi_i^{\alpha} \tag{3.2}$$

denote the L^2-approximation of the function v over the domain $\bar{\omega}_\alpha$.

Proposition 3.1. *It follows from the definition of the operator* Π_α^2 *that over the space* $\Xi_\alpha^{hp} \subset dom\Pi_\alpha^2$, *the operator reduces to the identity operator, i.e.,*

$$\forall g \in \Xi_\alpha^{hp}, \quad \Pi_\alpha^2 g = g,$$

that is, Π_α^2 *is a projection operator.*

Proof. The proof is immediate. Details can be found in [27]. ∎

Corollary 3.1. *The projection operator* Π_α^2 *preserves polynomials of degree* $\leq p$; *that is*

$$\Pi_\alpha^2 t = t \qquad \forall t \in \mathcal{P}_p(\omega_\alpha),$$

where p is the parameter that appears in the definition of the space Ξ_α^{hp}.

Proof. It follows immediately from previous proposition and Theorem 2.5. ∎

We say that the open set ω_α is affine equivalent to the open set $\hat{\omega}_\alpha$, if there is a mapping between ω_α and $\hat{\omega}_\alpha$ of the form

$$F_\alpha : \hat{\omega}_\alpha \to \omega_\alpha,$$

$$F_\alpha(\xi) = h_\alpha \xi + C, \qquad \xi \in \hat{\omega}_\alpha, \tag{3.3}$$

and $\forall y \in \omega_\alpha, \exists \xi \in \hat{\omega}_\alpha$ such that $y = F_\alpha(\xi)$.

Once we have established the bijection

$$\xi \in \hat{\omega}_\alpha \to y = F_\alpha(\xi) \in \omega_\alpha$$

between the points of the sets $\hat{\omega}_\alpha$ and ω_α, it is natural to associate the space

$$\hat{\Xi}_\alpha^{hp} := \{\hat{\Phi}_i^\alpha : \hat{\omega}_\alpha \to \mathbb{R} | \hat{\Phi}_i^\alpha = \Phi_i^\alpha \circ F_\alpha(\xi), \Phi_i^\alpha \in \Xi_\alpha^{hp}\}$$

with the space Ξ_α^{hp}.

With these definitions in mind, we are in a position to give the following definition:

Two balls $(\bar{\omega}_\alpha, \Xi_\alpha^{hp}, \mathbb{L}_\alpha^2)$ and $(\hat{\omega}_\alpha, \hat{\Xi}_\alpha^{hp}, \hat{\mathbb{L}}_\alpha^2)$ are said to be equivalent, if there is a mapping F_α between ω_α and $\hat{\omega}_\alpha$ such that the following relations hold:

(i) $\omega_\alpha = F_\alpha(\hat{\omega}_\alpha)$

(ii) $\Xi_\alpha^{hp} = \{\hat{\Phi}_i^\alpha : \hat{\omega}_\alpha \to \mathbb{R} | \hat{\Phi}_i^\alpha = \Phi_i^\alpha \circ F_\alpha(\xi), \Phi_i^\alpha \in \Xi_\alpha^{hp}\}$

(iii) $\hat{a}_l = a_l \qquad l \in I$,

where the functionals a_l are defined in (3.1) and $\hat{a}_l$ are given by

$$\hat{a}_l(\hat{v}) = \sum_{j \in I} (\hat{M}_{lj}^\alpha)^{-1} (\hat{v}, \hat{\Phi}_j^\alpha)_{L^2(\hat{\omega}_\alpha)}, \tag{3.4}$$

where

- $\hat{v} \in \hat{\Xi}_\alpha^{hp}$
- $\hat{M}_{lj}^\alpha = (\hat{\Phi}_l^\alpha \hat{\Phi}_j^\alpha)_{L^2(\hat{\omega}_\alpha)}$.

Theorem 3.1. *Let* $(\hat{\omega}_\alpha, \hat{\Xi}_\alpha^{hp}, \hat{\mathbb{L}}_\alpha^2)$ *and* $(\bar{\omega}_\alpha, \Xi_\alpha^{hp}, \mathbb{L}_\alpha^2)$ *be two equivalent balls with degrees of freedom in the form (3.1). Then if* $\hat{\Phi}_i^\alpha, i \in I$, *are the basis functions of the ball* $\hat{\omega}_\alpha$, *the functions* $\Phi_i^\alpha, i \in I$, *are the basis functions of the ball* ω_α, *the projection operators* Π_α^2 *and* $\hat{\Pi}_\alpha^2$ *are such that*

$$\widehat{\Pi_\alpha^2 v} = \hat{\Pi}_\alpha^2 \hat{v}$$

for any functions $\hat{v} \in dom\hat{\Pi}_\alpha^2$, *and* $v \in dom\Pi_\alpha^2$ *associated in the correspondence*

$$\hat{v} \in dom\hat{\Pi}_\alpha^2 \to v = \hat{v} \circ \boldsymbol{F}^{-1} \in dom\Pi_\alpha^2.$$

Proof. The L^2-approximation operator Π_α^2 is of the form

$$\Pi_\alpha^2 v = \sum_{k \in I} a_k(v)\Phi_i^\alpha,$$

where

$$a_k(v) = \sum_{j \in I} (\Phi_k^\alpha, \Phi_j^\alpha)_{L^2(\omega_\alpha)}^{-1} (v, \Phi_j^\alpha)_{L^2(\omega_\alpha)}$$

$$(\Phi_k^\alpha, \Phi_j^\alpha)_{L^2(\omega_\alpha)} = \int_{\omega_\alpha} \Phi_k^\alpha(y)\Phi_j^\alpha(y)dy = h^n \int_{\hat{\omega}_\alpha} \hat{\Phi}_k^\alpha(\xi)\hat{\Phi}_j^\alpha(\xi)d\xi$$

$$= h^n(\hat{\Phi}_k^\alpha, \hat{\Phi}_j^\alpha)_{L^2(\omega_\alpha)}$$

$$(v, \Phi_j^\alpha)_{L^2(\omega_\alpha)} = \int_{\omega_\alpha} v(y)\Phi_j^\alpha(y)dy = h^n \int_{\hat{\omega}_\alpha} \hat{v}(\xi)\hat{\Phi}_j^\alpha(\xi)d\xi$$

$$= h^n(\hat{v}, \hat{\Phi}_j^\alpha)_{L^2(\hat{\omega}_\alpha)}.$$

Thus,

$$a_k(v) = \sum_{j \in I} \frac{1}{h^n}(\hat{\Phi}_k^\alpha, \hat{\Phi}_j^\alpha)_{L^2(\hat{\omega}_\alpha)}^{-1} h^n(\hat{v}, \hat{\Phi}_j^\alpha)_{L^2(\hat{\omega}_\alpha)}$$

$$= \hat{a}_k(\hat{v}).$$

Then

$$(\Pi_\alpha^2 v)(y) = \sum_{k \in I} a_k(v)\Phi_k^\alpha(y) = \sum_{k \in I} \hat{a}_k(\hat{v})\Phi_k^\alpha(y)$$

$$(\widehat{\Pi_\alpha^2 v})(\xi) = (\Pi_\alpha^2 v) \circ \boldsymbol{F}_\alpha(\xi) = \sum_{k \in I} \hat{a}_k(\hat{v})\Phi_k^\alpha \circ \boldsymbol{F}_\alpha(\xi)$$

$$= \sum_{k \in I} \hat{a}_k(\hat{v})\hat{\Phi}_k^\alpha(\xi) = \hat{\Pi}_\alpha^2\hat{v}(\xi).$$

The next theorem is useful later on.   ■

Theorem 3.2.   *[32] Let* $W^{p+1,r}(\Omega) \hookrightarrow W^{m,s}(\Omega)$ *and let* $\Pi \in \mathcal{L}(W^{p+1,r}(\Omega), W^{m,s}(\Omega))$ *be a linear continuous operator from* $W^{p+1,r}(\Omega)$ *onto* $W^{m,s}(\Omega)$, *which preserves polynomials of degree* $\leq p$; *that is*

$$\Pi t = t \qquad \forall t \in \mathcal{P}_p(\Omega).$$

Then there exists a constant $C = C(\Omega)$ *such that, for every* $v \in W^{p+1,r}(\Omega)$,

$$|v - \Pi v|_{m,s,\Omega} \leq C(\Omega)\|I - \Pi\|_{\mathcal{L}(W^{p+1,r}(\Omega),W^{m,s}(\Omega))}|v|_{p+1,r,\Omega}.$$

Proof. See [32].   ■

Theorem 3.3. *Let ω_α and $\hat{\omega}_\alpha$ be two equivalent open sets in $\mathbb{R}^n$. If a function $v \in W^{m,s}(\omega_\alpha)$ for some integer $m \geq 0$ and some number $s \geq 1$, the function $\hat{v} = v \circ \mathbf{F}_\alpha$ belongs to the space $W^{m,s}(\hat{\omega}_\alpha)$, and, in addition, $\forall\, v \in W^{m,s}(\omega_\alpha)$ the following holds:*

$$|\hat{v}|_{m,s,\hat{\omega}_\alpha} = h_\alpha^{m-n/s}|v|_{m,s,\omega_\alpha},$$

where h_α is the parameter appearing in the mapping $\mathbf{F}_\alpha(\xi) = h_\alpha\xi + C, \xi \in \hat{\omega}_\alpha$.
Analogously, one has $\forall\, \hat{v} \in W^{m,s}(\hat{\omega}_\alpha)$

$$|v|_{m,s,\omega_\alpha} = h_\alpha^{-m+n/s}|\hat{v}|_{m,s,\hat{\omega}_\alpha}.$$

Proof. The proof involves standard algebraic manipulations. The details can be found in [27, 32]. ∎

We are now in a position to prove an important property of polynomial preserving operators. The key idea is to go from an open set Ω to an equivalent set $\hat{\Omega}$, and then go back to Ω. The following theorem is restricted to the case of maps defined in (3.3), which is the kind of mappings we are interested on. A more general version of it can be found in [31].

Theorem 3.4. *For some integers $p \geq 0$ and $m \geq 0$ and some numbers $r, s \in [1, \infty]$, let $W^{p+1,r}(\hat{\Omega})$ and $W^{m,s}(\hat{\Omega})$ be Sobolev spaces satisfying the inclusion*

$$W^{p+1,r}(\hat{\Omega}) \hookrightarrow W^{m,s}(\hat{\Omega}),$$

and let $\hat{\Pi} \in \mathcal{L}(W^{p+1,r}(\hat{\Omega}), W^{m,s}(\hat{\Omega}))$ be a mapping such that

$$\forall\, \hat{t} \in \mathcal{P}_p(\hat{\Omega}) \qquad \hat{\Pi}\hat{t} = \hat{t}.$$

For any open set Ω, which is equivalent to $\hat{\Omega}$, let the mapping $\Pi_\Omega v$ be defined by

$$(\widehat{\Pi_\Omega v}) = \hat{\Pi}\hat{v} \tag{3.5}$$

for all functions $\hat{v} \in W^{p+1,r}(\hat{\Omega})$ and $v \in W^{m,s}(\hat{\Omega})$ in the correspondence

$$\hat{v} = v \circ \mathbf{F}(\xi) \qquad \mathbf{F}(\xi) = h\xi + C. \tag{3.6}$$

Then there exists a constant $C(\hat{\Pi}, \hat{\Omega})$ such that, for all equivalent sets $\Omega, \forall\, v \in W^{p+1,r}(\Omega)$,

$$|v - \Pi_\Omega v|_{m,s,\Omega} \leq C(\hat{\Pi}, \hat{\Omega})h^{p+1-m+n/s-n/r}|v|_{p+1,r,\Omega}, \tag{3.7}$$

with h given by (3.6).
Proof. See [27, 31]. ∎

C. Estimates of the Approximation Error $|v - \Pi_\alpha^2 v|_{m,s,\omega_\alpha}$ for a Ball

By specializing Theorem 3.4 to balls, we obtain estimates of the approximation error $|v - \Pi_\alpha^2 v|_{m,s,\omega_\alpha}$. Before that we need a few more results.

Theorem 3.5. *The linear mapping $\hat{\Pi}_\alpha^2 : W^{p+1,r}(\hat{\omega}_\alpha) \to W^{m,s}(\hat{\omega}_\alpha)$ (the space $\hat{\Xi}_\alpha^{h,p}$ is contained in the space $W^{m,s}(\hat{\omega}_\alpha)$) is continuous.*
Proof. Let $\hat{v} \in W^{p+1,r}(\hat{\omega}_\alpha)$ then, from the definition of $\hat{\Pi}_\alpha^2$,

$$(\hat{\Pi}_\alpha^2\hat{v})(\xi) = \sum_{l \in I} \hat{a}_l(\hat{v})\hat{\Phi}_l^\alpha(\xi),$$

where

$$\hat{a}_l(\hat{v}) = \sum_{j \in I} (\hat{M}_{lj})^{-1} (\hat{v}, \hat{\Phi}_j^\alpha)_{L^2(\hat{\omega}_\alpha)}$$

and

$$\hat{M}_{lj}^\alpha = (\hat{\Phi}_l^\alpha, \hat{\Phi}_j^\alpha)_{L^2(\hat{\omega}_\alpha)}.$$

Thus,

$$
\begin{aligned}
\|\hat{\Pi}_\alpha^2 \hat{v}\|_{m,s,\hat{\omega}_\alpha} &\leq \sum_{l \in I} |\hat{a}_l| \|\hat{\Phi}_l^\alpha\|_{m,s,\hat{\omega}_\alpha} \\
&= \sum_{l \in I} |\sum_{j \in I} (\hat{M}_{lj})^{-1} (\hat{v}, \hat{\Phi}_j^\alpha)_{L^2(\hat{\omega}_\alpha)}| \|\hat{\Phi}_l^\alpha\|_{m,s,\hat{\omega}_\alpha} \\
&\leq \sum_{l \in I} \sum_{j \in I} |\hat{M}_{lj}|^{-1} \|\hat{\Phi}_j^\alpha\|_{L^2(\hat{\omega}_\alpha)} \|\hat{\Phi}_l^\alpha\|_{m,s,\hat{\omega}_\alpha} \|\hat{v}\|_{L^2(\hat{\omega}_\alpha)} \\
&\leq \left(\sum_{l \in I} \sum_{j \in I} |\hat{M}_{lj}|^{-1} \|\hat{\Phi}_j^\alpha\|_{L^2(\hat{\omega}_\alpha)} \|\hat{\Phi}_l^\alpha\|_{m,s,\hat{\omega}_\alpha} \right) \|\hat{v}\|_{p+1,r,\hat{\omega}_\alpha}.
\end{aligned}
$$

Assume, without loss of generality, that the functions $\Phi_l^\alpha, l \in I$, have been orthonormalized with respect to the inner product $(., .)_{L^2(\hat{\omega}_\alpha)}$. This implies that

$$\hat{M}_{lj} = \delta_{lj} = (\hat{M}_{lj})^{-1}$$

and

$$\sum_{l \in I} \sum_{j \in I} |\hat{M}_{lj}^{-1}| = \sum_{l \in I} \sum_{j \in I} \delta_{lj} = \dim(\hat{\Xi}_\alpha^{hp}).$$

This leads us to an interesting observation: If we use only the family $\mathcal{F}_N^{k,p=k}$, that is, only the partition of unity functions φ_α's, the dimension of the space $\hat{\Xi}_\alpha^{hp}$ is independent of k (the degree of the polynomial that the functions φ_α can reproduce). On the other hand, if we use the family $\mathcal{F}_N^{k,p}, p > k$, the dimension of the space $\hat{\Xi}_\alpha^{hp}$ will increase as we increase p and keep k fixed. Thus, we can write

$$\sum_{l \in I} \sum_{j \in I} |\hat{M}_{lj}^{-1}| \leq C(p).$$

Note that C is independent of k.

Collecting everything we get

$$\|\hat{\Pi}_\alpha^2 \hat{v}\|_{m,s,\hat{\omega}_\alpha} \leq C(\hat{\Omega}, p, \hat{\Pi}_\alpha^2) \|\hat{v}\|_{p+1,r,\hat{\omega}_\alpha}.$$

∎

Theorem 3.6. *Let $(\hat{\omega}_\alpha, \hat{\Xi}_\alpha^{hp}, \hat{\mathbb{L}}_\alpha^2)$ be a ball with $\hat{\Xi}_\alpha^{hp}$ and $\hat{\mathbb{L}}_\alpha^2$ defined as before. Suppose that the following holds for some integers $m \geq 0, p \geq 0$, and for some numbers $r, s \in [1, \infty]$:*

$$W^{p+1,r}(\hat{\omega}_\alpha) \hookrightarrow W^{m,s}(\hat{\omega}_\alpha)$$

$$\mathcal{P}_p(\hat{\omega}_\alpha) \subset \hat{\Xi}_\alpha^{hp} \subset W^{m,s}(\hat{\omega}_\alpha).$$

Then there exists a constant $C(\hat{\omega}_\alpha, \hat{\Xi}_\alpha^{hp}(p), \hat{\mathbb{L}}_\alpha^2)$ *such that, for the equivalent ball* $(\omega_\alpha, \Xi_\alpha^{hp}(p), \mathbb{L}_\alpha^2)$ *and all functions* $v \in W^{p+1,r}(\omega_\alpha)$,

$$|v - \Pi_\alpha^2 v|_{m,s,\omega_\alpha} \leq C(\hat{\omega}_\alpha, \hat{\Xi}_\alpha^{hp}(p), \hat{\mathbb{L}}_\alpha^2) h_\alpha^{p+1-m+n/s-n/r}|v|_{p+1,r,\omega_\alpha}, \qquad (3.8)$$

where h_α *is the parameter that appears in the mapping between* $\hat{\omega}_\alpha$ *and* ω_α.

Proof. By Corollary 3.1 we have that

$$\forall \hat{t} \in \mathcal{P}_p(\hat{\omega}_\alpha) \qquad \hat{\Pi}_\alpha^2 \hat{t} = \hat{t}.$$

Also, by Theorem 3.5 we have that

$$\hat{\Pi}_\alpha^2 \in \mathcal{L}(W^{p+1,r}(\hat{\omega}_\alpha), W^{m,s}(\hat{\omega}_\alpha)).$$

Since the projection operators Π_α^2 and $\hat{\Pi}_\alpha^2$ are related through the correspondence

$$\widehat{\Pi_\alpha^2 v} = \hat{\Pi}_\alpha^2 \hat{v}$$

for any functions $v \in \mathrm{dom}\Pi_\alpha^2$ and $\hat{v} \in \mathrm{dom}\hat{\Pi}_\alpha^2$ (cf. Theorem 3.1), we may apply Theorem 3.4, and inequality (3.8) is just a restatement of inequality (3.7) in the present case. ∎

Note that:

(i)   The rate of convergence given by (3.8) does not depend on the polynomial degree that the partition of unity functions can reproduce, but only on the degree p that the functions Φ_i^α can reproduce. That is, the rate given by the h-refinement using the family $\mathcal{F}_N^{k_1,p}$ is the same as the rate using the family $\mathcal{F}_N^{k_2,p}$. This is in agreement with our numerical experiments of Section IV. Note, however, that the definition of the families $\mathcal{F}_N^{k,p}$ implies that $p \geq k$. If $p = k$, then the rate of convergence is given by the polynomial degree that the partition of unity can reproduce.

(ii) The constant that appears in the inequality (3.8) does not depend on the polynomial degree that the partition of unity functions can reproduce, but only on the degree that the functions Φ_i^α can reproduce. This indicates that p-refinement using only moving least squares functions will probably not decrease the approximation error. Again, this is in agreement with our numerical experiments of Section IV.

(iii) There is no aspect ratio effect in the inequality (3.8), unlike in the finite element method. This phenomenon has been reported by Belytschko and colleagues in the element-free Galerkin method [1, 10], which is a special case of the h-p cloud method. This is a consequence of the kind of mappings used between the master ball $\hat{\omega}_\alpha$ and the balls ω_α.

D. Global Estimates

In this section, we present an estimate of the difference $(u - u_{hp})$, where $u \in H^l(\Omega), l \geq 1$, and u_{hp} is an approximation of u built using h-p cloud methods and belonging to a subspace X^{hp} of $H^1(\Omega)$. The approach used to derive the estimate follows that of Babuška and Rheinboldt [33] and of Melenk [34].

The proofs are given for the case where the partition of unity $\{\varphi_\alpha\}_{\alpha=1}^N$ is built using only the constant 1, that is, the case $k = 0$ in the definition given by (2.5). This does not represent a limitation in practice, since the numerical experiments of Section IV show that the case $k = 0$ is indeed the best choice for the h-p cloud method.

Let $\tilde{X}_\alpha^{hp}(\omega_\alpha^h)$ denote a two-parameter family of spaces defined by

$$\tilde{X}_\alpha^{hp}(\omega_\alpha^h) := \mathrm{span}\{\hat{L}_i \circ F_\alpha^{-1}\}_{i=1}^{D(v,p)}.$$

The mapping $\boldsymbol{F}_\alpha$ is defined in (3.3) and the basis functions $\hat{L}_i$ are chosen such that the following conditions are satisfied:

$$\hat{L}_1(x) \equiv 1$$

$$\mathcal{P}_p(\omega_\alpha) \subset \tilde{\boldsymbol{X}}_\alpha^{hp}(\omega_\alpha^h).$$

$D(n,p)$ depends on the choice of the set $\{\hat{L}_i\}$. If, for example, $\hat{L}_i$ are tensor product polynomials in $\mathbb{R}^n$, then

$$D(n,p) = (p+1)^n.$$

The restriction of the elements of $\tilde{\boldsymbol{X}}_\alpha^{hp}$ to $(\Omega \cap \omega_\alpha^h)$ are denoted by $\boldsymbol{X}_\alpha^{hp}$.

Definition 3.1.   *Let* $\Omega \subset \mathbb{R}^n$ *be an open set and* $\mathcal{T}_{N(h)} = \{\omega_\alpha^h\}_{\alpha=1}^{N(h)}, h > 0,$ *be a one-parameter family of open coverings of* Ω, *where*

$$\max_{\alpha=1,\ldots,N(h)} h_\alpha \leq h,$$

and h_α *is the radius of the ball* ω_α^h. *The family* $\mathcal{T}_{N(h)}$ *is said to satisfy the overlapping condition if* $\exists \rho \in \mathbb{N}$ *such that* $\forall h > 0$ *and* $\forall x \in \Omega$

$$card\{\alpha : x \in \omega_\alpha^h\} \leq \rho.$$

We associate with the family of open coverings $\mathcal{T}_{N(h)}$ a family of partitions of unity $\{\varphi_\alpha^h\}_{\alpha=1}^{N(h)}$ built using only the constant 1 ($k = 0$). The index h is used to emphasize that $\{\varphi_\alpha^h\}_{\alpha=1}^{N(h)}$ is an element of a family of partitions of unity.

Assumption 3.1.   *The family of partitions of unity* $\{\varphi_\alpha^h\}_{\alpha=1}^{N(h)}$ *satisfy the following additional conditions:*

1) $\|\varphi_\alpha^h\|_{L^\infty(\Omega)} \leq C_\infty$
2) $\|\nabla\varphi_\alpha^h\|_{L^\infty(\Omega)} \leq \frac{C_G}{h_\alpha}$

for some $C_\infty, C_G > 0$ *independent of* h.

Definition 3.2.   *Let* $\boldsymbol{X}_\alpha^{hp} \subset H^1(\Omega \cap \omega_\alpha^h)$ *be the two-parameter family of spaces defined above. The space* $\boldsymbol{X}^{hp}$ *is defined by*

$$\boldsymbol{X}^{hp} := \left\{ u_{hp} = \sum_{\alpha=1}^{N(h)} \varphi_\alpha^h u_\alpha^{hp} : u_\alpha^{hp} \in \boldsymbol{X}_\alpha^{hp} \right\}.$$

Lemma 3.1. $\boldsymbol{X}^{hp} = \text{span}\{\mathcal{F}_{N(h)}^{k=0,p}\}.$

   Proof.   From the definition of $\boldsymbol{X}^{hp}$ we have that

$$u_{hp} = \sum_{\alpha=1}^{N(h)} \varphi_\alpha^h u_\alpha^{hp}$$

$$= \sum_{\alpha=1}^{N(h)} \sum_{i=1}^{D(n,p)} a_{i\alpha}\varphi_\alpha^h(x)\hat{L}_i\left(\frac{x - x_\alpha}{h_\alpha}\right) \qquad \forall u_{hp} \in \boldsymbol{X}^{hp},$$

where $\hat{L}_1 \equiv 1$.

Consequently,

$$
\boldsymbol{X}^{hp} = \operatorname{span}\left\{
\begin{array}{cccc}
\varphi_1^h 1, & \varphi_2^h 1, & \cdots, & \varphi_{N(h)}^h 1, \\
\varphi_1^h \hat{L}_2\left(\frac{x-x_1}{h_1}\right), & \varphi_2^h \hat{L}_2\left(\frac{x-x_2}{h_2}\right), & \cdots, & \varphi_{N(h)}^h \hat{L}_2\left(\frac{x-x_{N(h)}}{h_{N(h)}}\right), \\
\varphi_1^h \hat{L}_3\left(\frac{x-x_1}{h_1}\right), & \varphi_2^h \hat{L}_3\left(\frac{x-x_2}{h_2}\right), & \cdots, & \varphi_{N(h)}^h \hat{L}_3\left(\frac{x-x_{N(h)}}{h_{N(h)}}\right), \\
\vdots & \vdots & \ddots & \vdots \\
\varphi_1^h \hat{L}_D\left(\frac{x-x_1}{h_1}\right), & \varphi_2^h \hat{L}_D\left(\frac{x-x_2}{h_2}\right), & \cdots, & \varphi_{N(h)}^h \hat{L}_D\left(\frac{x-x_{N(h)}}{h_{N(h)}}\right)
\end{array}
\right\}
$$

$$
= \operatorname{span}\{\mathcal{F}_{N(h)}^{k=0,p}\}.
$$

■

Theorem 3.7 [34]. *Let* $\Omega, \mathcal{T}_{N(h)} = \{\omega_\alpha^h\}_{\alpha=1}^{N(h)}, \{\varphi_\alpha^h\}_{\alpha=1}^{N(h)}$, *and* $\boldsymbol{X}_\alpha^{hp}$ *be as defined above. Let* $u \in H^l(\Omega), l \geq 1$, *and suppose that for fixed h and p the function u can be approximated locally by functions in* $\boldsymbol{X}_\alpha^{hp}$, *i.e., for each* $\alpha \; \exists u_\alpha^{hp} \in \boldsymbol{X}_\alpha^{hp}$ *such that*

$$
\|u - u_\alpha^{hp}\|_{L^2(\Omega \cap \omega_\alpha^h)} \leq C_1(\alpha,h,p)\|u\|_{H^l(\Omega \cap \omega_\alpha^h)}
$$

$$
|u - u_\alpha^{hp}|_{H^1(\Omega \cap \omega_\alpha^h)} \leq C_2(\alpha,h,p)\|u\|_{H^l(\Omega \cap \omega_\alpha^h)}.
$$

Then $\exists u_{hp} \in \boldsymbol{X}^{hp}$ *such that*

$$
\|u - u_{hp}\|_{L^2(\Omega)} \leq \rho C_\infty \max_{\alpha=1,\dots,N(h)} C_1(\alpha,h,p)\|u\|_{H^l(\Omega)},
$$

$$
|u - u_{hp}|_{H^1(\Omega)} \leq \sqrt{2}\rho \max_{\alpha=1,\dots,N(h)} \left(\frac{C_G C_1(\alpha,h,p)}{h_\alpha} + C_\infty C_2(\alpha,h,p)\right)\|u\|_{H^l(\Omega)},
$$

where the constants C_∞ *and* C_G *were defined in Assumption 3.1.*

Proof. [26] From the definition of the space $\boldsymbol{X}^{hp}$ and the fact that $\{\varphi_\alpha^h\}_{\alpha=1}^{N(h)}$ form a partition of unity, we have

$$
\|u - u_{hp}\|_{L^2(\Omega)}^2 = \left\|\sum_{\alpha=1}^{N(h)} \varphi_\alpha^h(u - u_\alpha^{hp})\right\|_{L^2(\Omega)}^2 = \int_\Omega \left|\sum_{\alpha=1}^{N(h)} \varphi_\alpha^h(u - u_\alpha^{hp})\right|^2 d\Omega.
$$

Using the Schwarz inequality and the fact that for a fixed $x \in \Omega$ there are no more than ρ nonzero terms in the above sum, we get

$$
\int_\Omega \left|\sum_{\alpha=1}^{N(h)} \varphi_\alpha^h(u - u_\alpha^{hp})\right|^2 d\Omega \leq \rho \int_\Omega \sum_{\alpha=1}^{N(h)} |\varphi_\alpha^h(u - u_\alpha^{hp})|^2 d\Omega
$$

$$
\leq \rho C_\infty^2 \sum_{\alpha=1}^{N(h)} \int_{\Omega \cap \omega_\alpha^h} |u - u_\alpha^{hp}|^2 d\Omega
$$

$$
\leq \rho C_\infty^2 \sum_{\alpha=1}^{N(h)} C_1^2(\alpha,h,p)\|u\|_{H^l(\Omega \cap \omega_\alpha^h)}^2
$$

$$
\leq \rho C_\infty^2 \max_{\alpha=1,\dots,N(h)} C_1^2(\alpha,h,p)\rho\|u\|_{H^l(\Omega)}^2.
$$

■

The semi-norm estimate follows as above [27].

Suppose now that in Sections B and C we define $\Xi_\alpha^{hp} := X_\alpha^{hp}$, then we can carry over all the proofs given there, since as in the case of the space $\Xi_\alpha^{hp}, \mathcal{P}_p \subset X_\alpha^{hp}$. We then conclude the following theorem.

Theorem 3.8. *Suppose that the following holds for some integers* $m \geq 0, p \geq 0$ *and for some numbers* $r, s \in [1, \infty]$:

$$W^{p+1,r}(\widehat{\Omega \cap \omega_\alpha^h}) \hookrightarrow W^{m,s}(\widehat{\Omega \cap \omega_\alpha^h})$$

$$\mathcal{P}_p(\widehat{\Omega \cap \omega_\alpha^h}) \subset \hat{X}_\alpha^{hp} \subset W^{m,s}(\widehat{\Omega \cap \omega_\alpha^h}).$$

Let $(\widehat{\Omega \cap \omega_\alpha^h}, \hat{X}_\alpha^{hp}, \hat{\mathbb{L}}_\alpha^2)$ *be a ball with* $\hat{X}_\alpha^{hp}$ *and* $\hat{\mathbb{L}}_\alpha^2$ *defined as before. Then there exists a constant* $C(\widehat{\Omega \cap \omega_\alpha^h}, \hat{X}_\alpha^{hp}, \hat{\mathbb{L}}_\alpha^2)$ *such that, for any equivalent ball* $(\Omega \cap \omega_\alpha^h, X_\alpha^{hp}, \mathbb{L}_\alpha^2)$ *and all functions* $u \in W^{p+1,r}(\Omega \cap \omega_\alpha^h)$,

$$|u - \Pi_\alpha^2 u|_{m,s,(\Omega \cap \omega_\alpha^h)} \leq C(\widehat{\Omega \cap \omega_\alpha^h}, \hat{X}_\alpha^{hp}, \hat{\mathbb{L}}_\alpha^2) h_\alpha^{p+1-m+n/s-n/r} |u|_{p+1,r,(\Omega \cap \omega_\alpha^h)}, \quad (3.9)$$

where h_α *is the parameter that appears in the mapping between* $(\widehat{\Omega \cap \omega_\alpha^h})$ *and* $(\Omega \cap \omega_\alpha^h)$.

Theorem 3.9. *Suppose that the conditions of Theorem 3.8 hold for all master balls* $(\Omega \cap \omega_\alpha^h, \hat{X}_\alpha^{hp}, \hat{\mathbb{L}}_\alpha^2)$. *Let* $u \in H^{p+1}(\Omega), p \geq 0$, *then for fixed h and p there is* $u_{hp} \in X^{hp}$ *such that*

$$\|u - u_{hp}\|_{L^2(\Omega)} \leq \rho C_\infty \max_{\alpha=1,\ldots,N(h)} C_\alpha h^{p+1} \|u\|_{H^{p+1}(\Omega)},$$

$$|u - u_{hp}|_{H^1(\Omega)} \leq \sqrt{2}\rho \max_{\alpha=1,\ldots,N(h)} (C_G C_\alpha + C_\infty C_\alpha) h^p \|u\|_{H^{p+1}(\Omega)},$$

where the constants C_∞ *and* C_G *were defined in Assumption 3.1, the constant* $C_\alpha = C(\widehat{\Omega \cap \omega_\alpha^h}, \hat{X}_\alpha^{hp}, \hat{\mathbb{L}}_\alpha^2)$ *is the same as in Theorem 3.8, and* $h = \max_{\alpha=1,\ldots,N(h)} h_\alpha$.

Proof. The above relations are direct consequences of Theorems 3.7 and 3.8. ■

IV. NUMERICAL EXPERIMENTS

In this section we perform several numerical experiments to investigate the approximating properties of the *h-p* cloud functions introduced in previous sections. The *h* and *p* convergence of the method are investigated, and the results compared with the *a-priori* error estimate derived in the previous section.

In the *h* version of the method, the parameters *k* and *p* are kept fixed, and the size h_α of the balls ω_α are changed. Of course, this has to be followed by an increase in the number of nodes in the discretization when the sizes of the balls are decreased.

The *p* version of the method can have more than one variant. One, for example, can fix the size h_α of the balls and change the parameter *p* while keeping *k* fixed. Another possibility is to increase simultaneously *k* and *p*. Nonetheless, our analysis in Section III shows that the constant that appears in the error estimate given by Theorem 3.6 does not depend on *k*, but only on *p*. Thus, it may not be advantageous to increase the value of *k*.

In all the numerical experiments, the weighting functions $\mathcal{W}_\alpha$ are implemented using cubic B-splines in the following way:

$$\mathcal{W}_\alpha(y) := W_\alpha(z) := W(z_\alpha), \tag{4.1}$$

where

$$z_\alpha := \frac{2\|y - x_\alpha\|_{\mathbb{R}^n}}{h_\alpha} \equiv \frac{2\|r_\alpha\|_{\mathbb{R}^n}}{h_\alpha} \equiv \frac{2u_\alpha}{h_\alpha}$$

and

$$W(z_\alpha) := \begin{cases} \frac{C}{h_\alpha^n}\left[1 - \frac{3}{2}z_\alpha^2 + \frac{3}{4}z_\alpha^3\right] & \text{if } 0 \le z_\alpha < 1 \\ \frac{C}{4h_\alpha^n}[2 - z_\alpha]^3 & \text{if } 1 \le z_\alpha < 2 \\ 0 & \text{if } z_\alpha \ge 2, \end{cases} \tag{4.2}$$

where n is the dimension of the problem and C is a constant given by

$$C = \begin{cases} \frac{2}{3} & \text{if } n = 1 \\ \frac{10}{7\pi} & \text{if } n = 2 \\ \frac{1}{\pi} & \text{if } n = 3. \end{cases}$$

The derivatives of the weighting function are given by

$$\frac{\partial \mathcal{W}_\alpha}{\partial y_i} = \frac{dW}{dz_\alpha}\frac{\partial z_\alpha}{\partial y_i} = \frac{dW}{dz_\alpha}\frac{dz_\alpha}{u_\alpha}\frac{\partial u_\alpha}{\partial y_i} = \frac{dW}{dz_\alpha}\frac{2}{h_\alpha}\frac{r_i}{u_\alpha}, \tag{4.3}$$

where

$$\frac{dW}{dz_\alpha} = \begin{cases} \frac{3C}{h_\alpha^n}\left[-z_\alpha + \frac{3}{4}z_\alpha^2\right] & \text{if } 0 \le z_\alpha < 1 \\ \frac{-3C}{4h_\alpha^n}[2 - z_\alpha]^2 & \text{if } 1 \le z_\alpha < 2 \\ 0 & \text{if } z_\alpha \ge 2. \end{cases} \tag{4.4}$$

In all experiments done in this section and in Section V, the domain integrals are computed using a background cell structure that exactly covers the domain. In all cases, there is no relationship between the background cell structure and the set of nodes Q_N used in the discretizations.

A. Test 1: L^2 Projection of a Smooth Function in 1-D

We compute the L^2 projection, u_{hp}, of the function $u = \sin(4\pi x), x \in (0,1)$, on a subspace spanned by cloud functions. Many subfamilies of the general family $\mathcal{F}_N^{k,p}$ are tested. The results for the h and p convergence of these subfamilies are presented and analyzed next.

H Convergence

In this section we investigate the behavior of the error $u - u_{hp}$ in the L^2 norm when uniform h refinement is performed. The number of nodes ranges from 9-129, always evenly distributed in
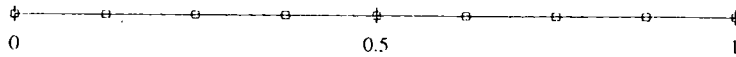

FIG. 6. Nine nodes arrangement for Test 1.

the interval $[0, 1]$ with one node at each end of the domain. The nine node distribution is shown in Fig. 6. In the experiments, k and p ranges from 0--2.

Figure 7(a) shows the h convergence, in the L^2 norm, of u_{hp}. The results are shown for three cases: $k = p = 0, k = p = 1$, and $k = p = 2$. The curves show that the rate of convergence is equal to $p + 1$, which is in agreement with the estimate given by Theorem 3.9.

Figure 7(b) shows the results when the basis functions from the spaces $\mathcal{F}_{9 \leq N \leq 129}^{k=0,p=0}$, $\mathcal{F}_{9 \leq N \leq 129}^{k=0,p=1}$, and $\mathcal{F}_{9 \leq N \leq 129}^{k=0,p=2}$ are used. That is, we compare the rates of convergence when different values of p are used and k is kept constant. The curves show that the rate of convergence is equal to $p + 1$, again in agreement with Theorem 3.9. Another test on the dependence of the rate of convergence on k and p was performed by comparing the rates of convergence when using different values of k while keeping p constant. The results are shown in Fig. 8(a). It can be observed that the rate of convergence is always approximately equal to $p + 1$ and does not depend on the value of k. Figure 8(b) shows the same results, but this time the error $u - u_{hp}$ is plotted against the number of degrees of freedom instead of the size of the balls. The conclusions in this case are the same as before.

P Convergence

In this section we analyze the effect of uniform p enrichment of the h-p cloud space on the error $u - u_{hp}$ measured in the L^2 and H^1 norms. More than one variant of the p version are investigated. We denote by variant $\wp_1$ the case when k and p are simultaneously increased and by variant $\wp_2$, the case when k is kept fixed while p is increased. In all experiments reported in this section, the nine node arrangement shown in Fig. 6 is used and the algorithm previously described is used to automatically set the size of the balls.
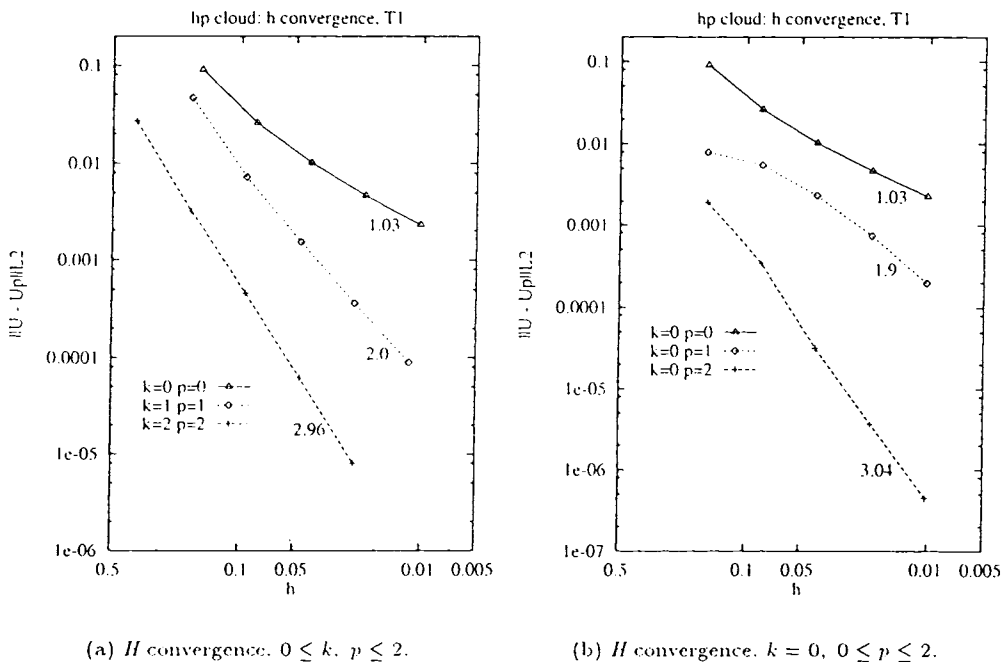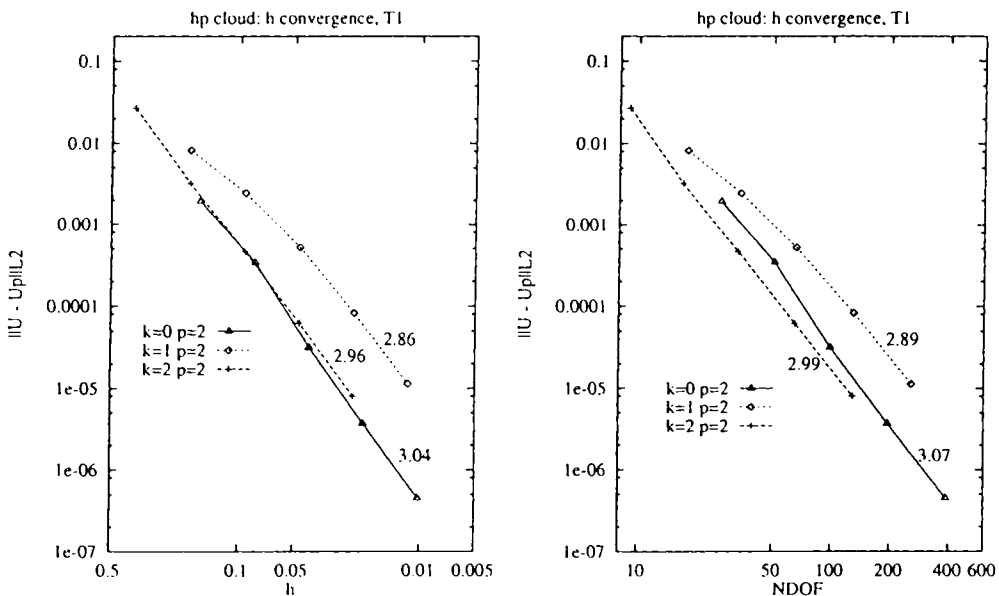

(a) H convergence. $0 \leq k$, $p \leq 2$.   (b) H convergence. $k = 0$, $0 \leq p \leq 2$.

FIG. 7. H convergence in the L^2 norm.

Figure 9(a) shows the results for the variant $\wp_1$ with $1 \le k = p \le 5$, and for the variant $\wp_2$ when $k = 0, 1 \le p \le 7; k = 1, 1 \le p \le 7$ and $k = 2, 2 \le p \le 7$. The variant $\wp_2$ with $k = 0$ gives, for all values of p, the smallest error. The rate of convergence increases with p in all experiments using the variant $\wp_2$. As Fig. 9(a) shows, the rate of convergence ranges from 2.02–17.26 when the variant $\wp_2$ with $k = 0$ is used. This behavior is typical of spectral methods like the p version of the finite element method. These results confirm the dependence on p of the constant that appears in the error estimate of theorem 3.9. The results obtained with variant $\wp_1$ are also shown in Fig. 9(a). It can be observed that this variant does not converge. This is probably a consequence that the constant of the error estimate (3.8) does not depend on k.

Figure 9(a) shows that for a fixed value of p the variant $\wp_2$ with $k = 0$ gives, for this problem, the smallest error. Nonetheless, it can not be concluded that the choice of $k = 0$ is the best in terms of error versus number of degrees of freedom. This happens because the definition of the family $\mathcal{F}_N^{k,p}$ given in (2.5) implies that $\dim\{\mathcal{F}_N^{k1,p}\} > \dim\{\mathcal{F}_N^{k2,p}\}$ if $k2 > k1$. Figure 9(b) shows the same results of Fig. 9(a), but this time we plot the error of the L^2 projection versus the number of degree of freedom. It can be observed that in all the cases ($k = 0, k = 1$ or $k = 2$) the error, for a fixed number of degrees of freedom, is almost the same, with only a slight advantage in favor of the case $k = 0$. We should now recall that the definition of the moving least squares (partition of unity) functions φ_α given by (2.3) involves the inversion of a matrix of dimensions $(\dim \mathbb{P}) \times (\dim \mathbb{P})$ and that $\dim \mathbb{P}$ is at least equal to $\binom{k+n}{k}$. Thus, we conclude that, for this problem, the family $\mathcal{F}_N^{k=0,p}$ is the most economical, since it does not involve the inversion of any matrix in the construction of the moving least squares functions φ_α and gives the same level of accuracy of the other families for a fixed number of degree of freedom. Figures 10(a) and 10(b) are similar to Figs. 9(a) and 9(b), respectively, but this time the error $u - u_{hp}$ is measured in the H^1 norm. The conclusions are the same as before.

(a) H convergence. $p = 2$, $0 \le k \le 2$.

(b) H convergence. $p = 2$, $0 \le k \le 2$.

FIG. 8. H convergence in the L^2 norm.

(a) P convergence. $0 \leq k \leq 2$, $1 \leq p \leq 7$.   (b) P convergence. $0 \leq k \leq 2$, $0 \leq p \leq 7$.
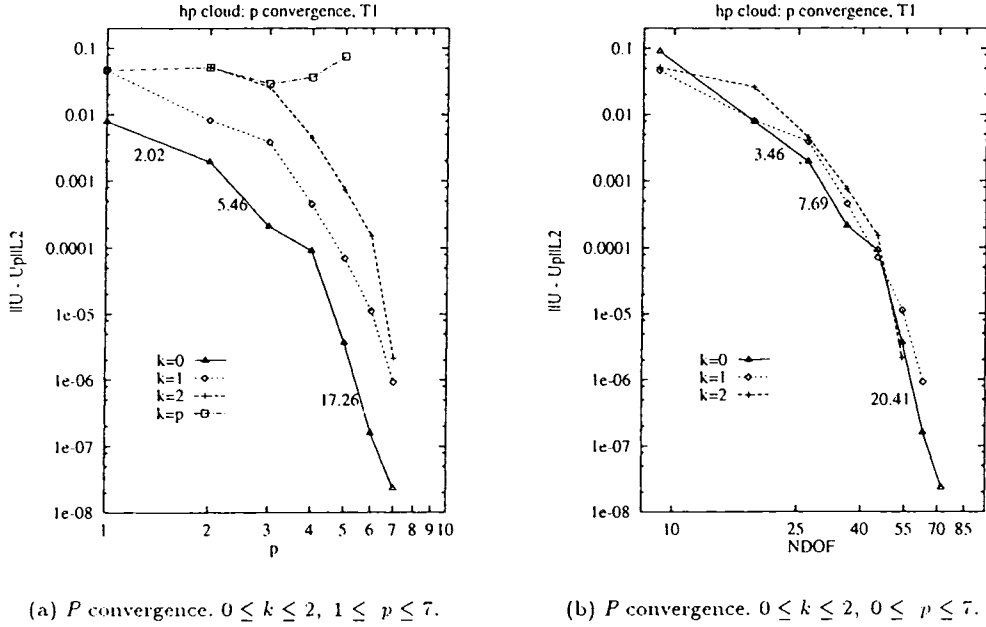
FIG. 9. P convergence in the L^2 norm.

B. Test 2: L^2 Projection of a Rough Function

We shall now illustrate the performance of the cloud functions in approximating a function with a high gradient in some small part of the domain. The model function is

$$u = (1 - x)[\tan^{-1}(\gamma(x - x_0)) + \tan^{-1}(\gamma x_0)]   \Omega = (0, 1).$$

We test the case $\gamma = 50$ (γ controls the magnitude of the gradient at x_0) with $x_0 = 0.2$. du/dx is shown in Fig. 12(a).

We perform a p convergence analysis using the variant $\wp_2$ and the same families used in the previous experiment. The nine node arrangement shown in Fig. 6 is also used in this experiment. Figure 12(b) shows the results when $k = 0, 1 \leq p \leq 7; k = 1, 1 \leq p \leq 7$ and $k = 2, 2 \leq p \leq 7$. Figure 13(a) shows the same results of Fig. 12(b) with the exception that the abscissa shows the number of degrees of freedom instead of the value of p. We can draw the same conclusions as in the previous test case, namely, we get spectral c onvergence with the rate of convergence ranging from 0.90 to 8.30, and the family $\mathcal{F}_N^{k=0,p}$ is the best choice.

We next investigate the possibility of getting even higher rates of convergence using a node distribution that takes into account the behavior of the function u around $x_0 = 0.2$. We use the graded node arrangement shown in Fig. 11. The results obtained are plotted against the previous ones in Fig. 13(b). We can observe a clear increase in the rate of convergence when the graded node distribution is used. The results shown are for the family $\mathcal{F}_N^{k=0,1\leq p \leq 7}$ with $N = 9$ (in the case of the uniform node arrangement) and $N = 29$ (in the case of the graded node arrangement).

The conclusion from this experiment is that, like in the finite element method, the use of adaptivity to automatically select the node arrangement and spectral orders in the h-p cloud method can possibly lead to substantial savings in computations.
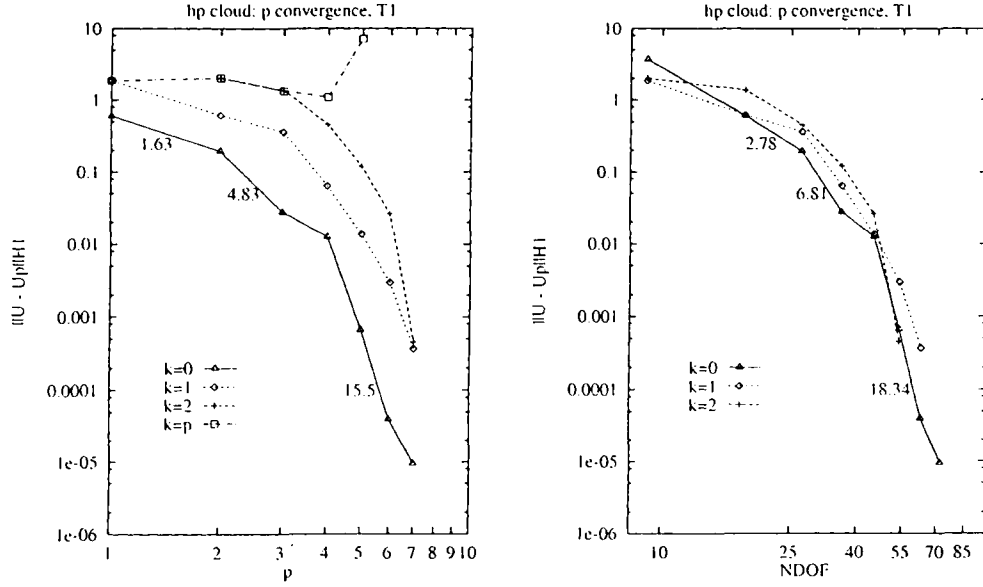
(a) P convergence. $0 \le k \le 2$, $1 \le p \le 7$. (b) P convergence. $0 \le k \le 2$, $0 \le p \le 7$.

FIG. 10. P convergence in the H^1 norm.

V. SOLUTION OF BVPS USING THE FAMILIES $\mathcal{F}_N^{K,P}$ AND THE GALERKIN METHOD - THE H-P CLOUD METHOD

A. Introduction

In the following sections, the h-p cloud method denotes a numerical technique to solve boundary-value problems, where one uses the h-p cloud functions to construct appropriate finite dimensional subspaces of functions used in a Galerkin method. The use of the Galerkin method is only a question of choice. Other techniques, such as collocation, can be used as well.

One- and two-dimensional boundary-value problems are solved using the h-p cloud method. Some of the results are compared with the solutions obtained using the FEM.

B. Heat Conduction Equation in One Dimension

The following boundary-value problem is solved using the p version of the h-p cloud method:
  Find $u = u(x)$ such that

$$-\frac{d^2u}{dx^2} = f \qquad \text{in } \Omega = (-1, 1)$$
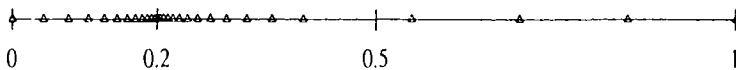$$u = u_1 \qquad \text{at } x = -1$$

FIG. 11. Graded node arrangement for Test 2.

$$\frac{du}{dx} = \sigma_2 \qquad \text{at } x = 1.$$

The parameters f, u_1, and σ_2 are chosen such that the solution u is given by

$$u = \frac{35}{8}x^4 - \frac{15}{4}x^2 + \frac{3}{8},$$

that is, the Legendre polynomial of fourth degree.

A five-node arrangement uniformly distributed in the domain is used in the computations. The value of the parameter k is kept fixed at zero, and the parameter p ranges from 0-3. The discretization using the family $\mathcal{F}_{N=5}^{k=0,p=4}$ gives, as expected, the exact solution within round-off and quadrature errors. The essential boundary condition at $x = -1$ is imposed using a Lagrange multiplier.

This problem is also solved using the p version of the finite element method. A uniform mesh of four elements is used in the discretization. The degree of the finite elements ranges from 1-3.

The first difficulty in comparing the h-p cloud method with the FEM is to decide how to do a fair comparison. One can compare based on the value of p or on the number of degrees of freedom. We compare the solutions corresponding to approximately the same number of degrees of freedom.

Figure 14(a) shows the pointwise error, $u_{,x} - u_{p,x}$, when using the h-p cloud method with $k = 0, p = 0$, and the FEM with $p = 1$. In both cases, the number of degrees of freedom is equal to 5. It can be observed that the error in the maximum norm is almost the same in both cases, but the derivative of the h-p cloud solution does not exhibit discontinuities like the derivative of the FE solution. The results when $k = 0, p = 1$ in the h-p cloud method, and $p = 2$ in the FEM are
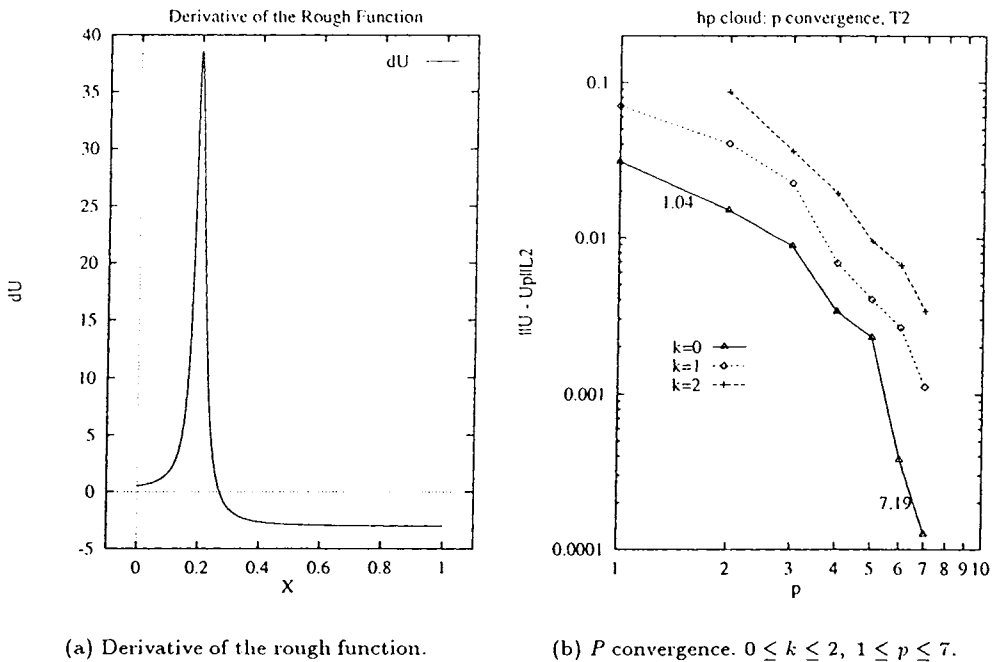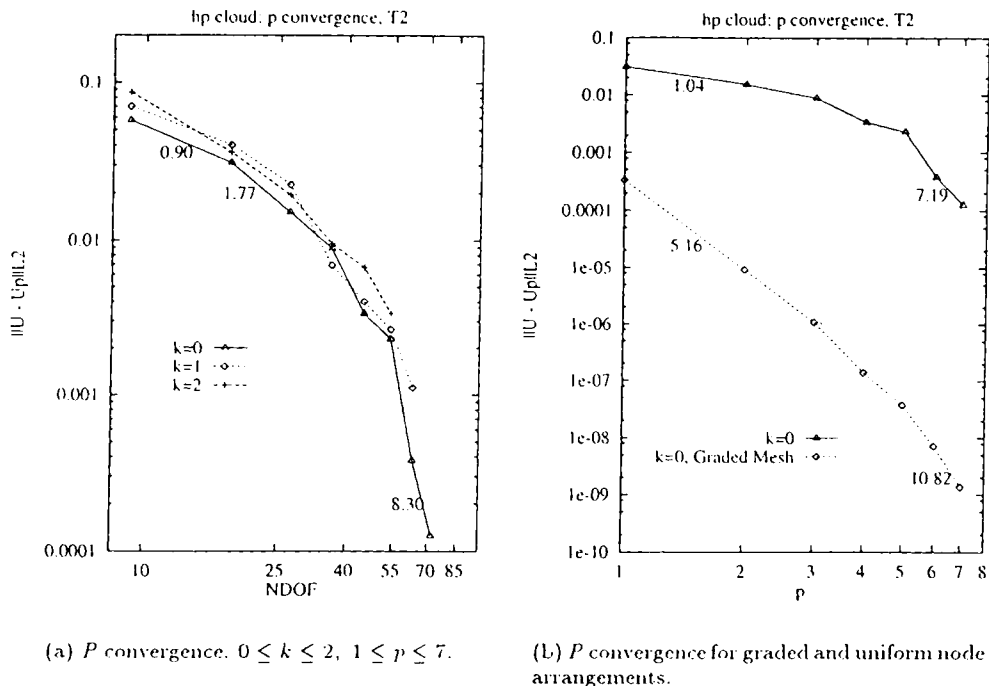

(a) Derivative of the rough function.   (b) P convergence. $0 \le k \le 2$, $1 \le p \le 7$.

FIG. 12.   Derivative of the rough function and p convergence in the L^2 norm.

(a) *P* convergence. $0 \leq k \leq 2$, $1 \leq p \leq 7$.

(b) *P* convergence for graded and uniform node arrangements.

FIG. 13. *P* convergence in the L^2 norm.

shown in Fig. 14(b). The error in the maximum norm of the h-p cloud flux is about three times smaller than the corresponding error of the FE flux. It can be observed that the h-p cloud solution is at least a $C^1(\Omega)$ function.
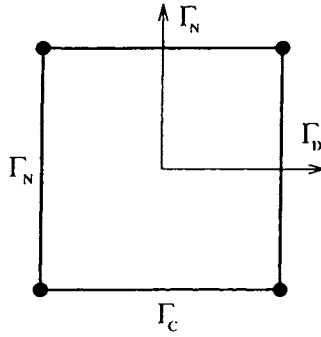

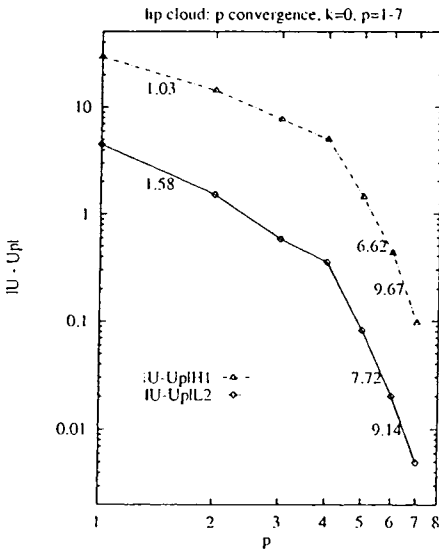(a)

(b)
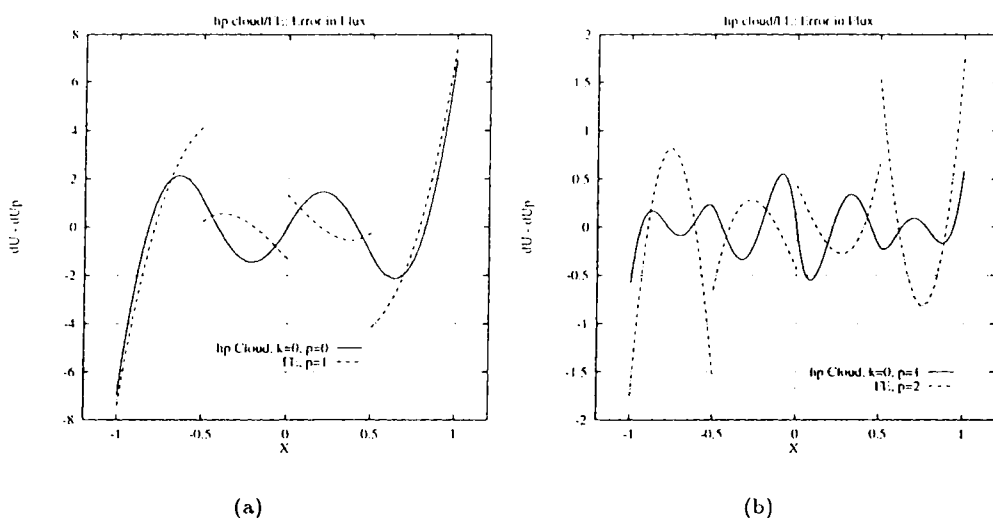
FIG. 14. *H*-*p* cloud and FE error in flux.

FIG. 15. Node arrangement.

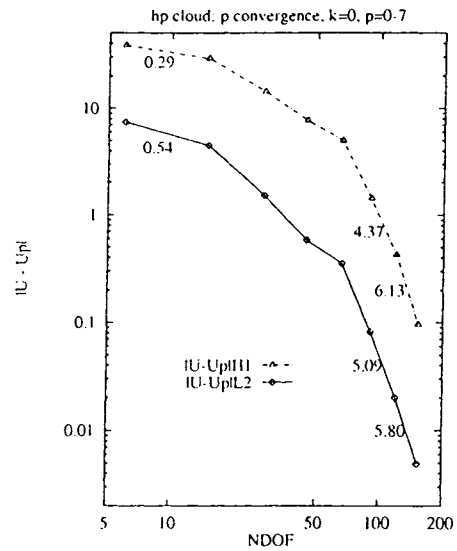## C. Poisson's Equation on a Square Domain

In this section, we focus on the solution of a Poisson problem in which a function $u = u(x)$ is sought satisfying

$$-\Delta u = f \qquad \text{in } \Omega = (-1,1) \times (-1,1)$$

$$-\frac{\partial u}{\partial n} = \hat{g} \qquad \text{on } \Gamma_N$$

$$-\frac{\partial u}{\partial n} = (u - u_\infty) \qquad \text{on } \Gamma_C$$

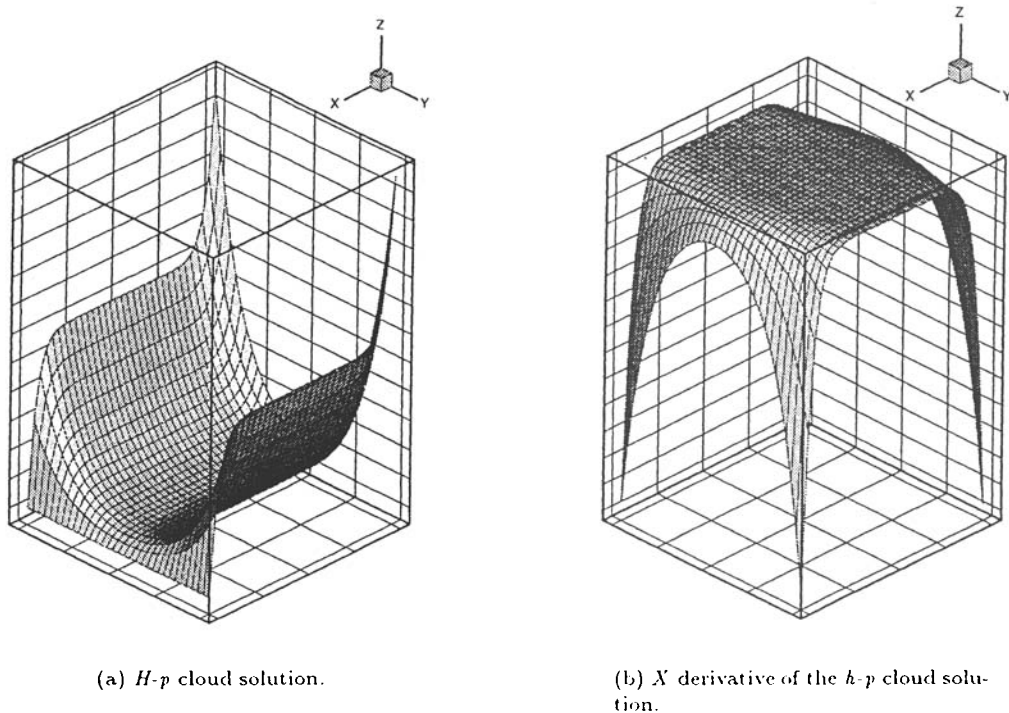$$u = 0 \qquad \text{on } \Gamma_D,$$

(a) P convergence, $k = 0$, $1 \le p \le 7$.

(b) P convergence, $k = 0$, $0 \le p \le 7$.

FIG. 16. P convergence in the L^2 and H^1 norms.

(a) H-p cloud solution.

(b) X derivative of the h-p cloud solution.

FIG. 17. H-p cloud solution and x derivative of the h-p cloud solution.

where Δ is the Laplacian, and $f, \hat{g}$, and $u_{\times}$ are chosen such that the solution u is

$$u = (1 - x^{11}) \cos h(\pi y).$$

The domain Ω and the node arrangement used are represented in Fig. 15.

This problem is solved using its weak formulation and the Galerkin method. The subspaces for the Galerkin method are built using the h-p cloud functions described in previous sections. The Dirichlet boundary condition is imposed using Lagrange multipliers. Details on the implementation of the Lagrange multipliers can be found in, e.g., [10].

The variant $\wp_2$ of the p version of the h-p cloud method is used. The value of k is kept fixed at $k = 0$ and p ranges from 0 to 7. Figure 16(a) shows the error $u - u_p$, measured in the H^1 and L^2 norms, versus the value of p. The rate of convergence in the L^2 norm ranges from 1.58–9.14 and, in the H^1 norm, it ranges from 1.03–9.67. This kind of behavior is typical of spectral methods. Figure 16(b) shows the error $u - u_p$ versus the total number of degrees of freedom (including the degrees of freedom corresponding to the Lagrange multipliers).

Figure 17(a) shows the h-p cloud solution u_p and Fig. 17(b) shows its x derivative. It can be observed that $\partial u_p / \partial x$ is continuous, and it is, therefore, unnecessary to perform any flux smoothing.

VI. CONCLUSIONS

In this article, a new meshless method to solve a large class of boundary-value problems is proposed. The method involves the placement of h-p approximations in spheres centered at arbitrary points in the domain. The method can be used in one, two, as well as three dimensions. *a-priori* error estimates for the h version of the method are derived. The method appears to be robust enough to handle problems where the solution exhibits localized behavior, such as boundary layers. The numerical experiments show that one can expect exponential rates of convergence when the h-p version of the method is used. Another remarkable feature of the h-p cloud method is the regularity of the solution one can get. We were able to obtain $C^2(\Omega)$ approximate solutions of a second-order boundary-value problem without any difficulty. Higher-order of regularity can be attained at no extra cost.

Much additional work remains to be done, but the results presented in this article show that the h-p cloud method has a great potential to become a very competitive method for the solution of a broad class of boundary-value problems.

References

1. T. Belytschko, Y. Y. Lu, and L. Gu, "Crack propagation by element free Galerkin methods," in *Advanced Computational Methods for Material Modeling*, p. 191, 1993. AMD-Vol. 180/PVP-Vol. 268, ASME 1993.

2. Tadeusz Liszka, "An interpolation method for an irregular net of nodes," *Inter. J. Numer. Meth. Eng.* **20,** 1599 (1984).

3. Tadeusz Liszka and J. Orkisz, "Finite difference method for arbitrary irregular meshes in nonlinear problems of applied mechanics," in *IV SMiRt*, San Francisco, 1977.

4. Tadeusz Liszka and J. Orkisz, "The finite difference method at arbitrary irregular grids and its application in applied mechanics," *Comput. Struct.* **11,** 83 (1980).

5. R. A. Gingold and J. J. Monaghan, "Kernel estimates as a basis for general particle methods in hydrodynamics," *J. Comp. Phys.* **46,** 429 (1982).

6. L. B. Lucy, "A numerical approach to the testing of the fission hypothesis," *Astron. J.* **82,** 1013 (1977).

7. J. J. Monaghan, "Why particle methods work," *SIAM J. Sci. Stat. Comput.* **3,** 422 (1982).

8. J. J. Monaghan, "An introduction to sph," *Comp. Phys. Comm.* **48,** 89 (1988).

9. B. Nayroles, G. Touzot, and P. Villon, "Generalizing the finite element method: Diffuse approximation and diffuse elements," *Comp. Mech.* **10,** 307 (1992).

10. T. Belytschko, Y. Y. Lu, and L. Gu, "Element-free Galerkin methods," *Int. J. Num. Meth. Eng.* **37,** 229 (1994).

11. K. Amarantuga, J. R. Williams, S. Qian, and J. Weis, "Wavelet–Galerkin solutions for one-dimensional partial differential equations," *Int. J. Num. Meth. Eng.* **37,** 2703 (1994).

12. R. Glowinski, M. Lawton, M. Ravachol, and E. Tenenbaum, "Wavelet solutions of linear and nonlinear elliptic, parabolic and hyperbolic problems in one space dimension," in *9th Int. Conf. on Numerical Methods in Applied Sciences and Engineering*, SIAM, Philadelphia, 1990.

13. Sam Qian and J. Weiss, ''Wavelet and the numerical solution of partial differential equations,'' *J. Comp. Phys.* **106,** 155 (1993).

14. E. J. Kansa, ''Multiquadrics—a scattered data approximation scheme with applications to computational fluid-dynamics—i surface approximations and partial derivative estimates,'' *Comput. Math. Appl.* **19,** 127 (1990).

15. E. J. Kansa, ''Multiquadrics—a scattered data approximation scheme with applications to computational fluid-dynamics—ii solutions to parabolic, hyperbolic and elliptic partial differential equations,'' *Comput. Math. Appl.* **19,** 147 (1990).

16. Wing Kam Liu and Yijung Chen, ''Wavelet and multiple scale reproducing kernel methods,'' *Inter. J. Num. Meth. Fluids,* to appear.

17. Wing Kam Liu, Sukky Jun, Shaofan Li, Jonathan Adee, and Ted Belytschko, ''Reproducing kernel particle methods for structural dynamics,'' *Inter. J. Num. Meth. Eng.,* to appear.

18. Genki Yagawa, ''Some remarks on free mesh method: A kind of meshless finite element method,'' in *International Conference on Computational Engineering Science,* Hawaii, August 1995.

19. P. Lancaster and K. Salkauskas, ''Surfaces generated by moving least squares methods,'' *Math. Comp.* **37,** 141 (1981).

20. P. Lancaster and K. Salkauskas, *Curve and Surface Fitting, an Introduction,* Academic Press, San Diego, 1986.

21. C. A. M. Duarte, ''A review of some meshless methods to solve partial differential equations,'' *Technical Report 95-06,* TICAM, The University of Texas at Austin, 1995.

22. J. W. Swegle, S. W. Attaway, M. W. Heinstein, F. J. Mello, and D. L. Hicks, ''An analysis of the smoothed particle hydrodynamics,'' *Technical Report SAND93-2513 UC-705,* Sandia, 1994.

23. Y. Y. Lu, Ted Belytschko, and M. Tabbara, ''Element-free Galerkin method for wave propagation and dynamic fracture,'' *Comput. Meth. Appl. Mech. Eng.,* to appear.

24. Richard Franke, ''Scattered data interpolation: Test of some methods,'' *Math. Comp.* **38,** 181 (1982).

25. Y. Y. Lu, T. Belytschko, and L. Gu, ''A new implementation of the element free Galerkin method,'' *Comput. Meth. Appl. Mech. Eng.* **113,** 397 (1994).

26. Mark Ainsworth, Personal communication, 1994.

27. C. A. M. Duarte and J. T. Oden, ''Hp clouds—a meshless method to solve boundary-value problems'' *Technical Report 95-05,* TICAM, The University of Texas at Austin, 1995.

28. R. Adams, *Sobolev Spaces.* Academic Press, Boston, 1978.

29. D. Shepard, ''A two-dimensional function for irregularly spaced data,'' in *ACM Nat. Conf.* p. 517, 1968.

30. T. Belytschko and S. Beissel, ''Nodal integration of the element-free Galerkin method,'' pre-print, 1995.

31. Philippe G. Ciarlet, *The Finite Element Method for Elliptic Problems,* North–Holland, Amsterdam, 1978.

32. J. T. Oden and G. F. Carey, *Texas Finite Element Series Volume IV—Mathematical Aspects,* Prentice–Hall, New Jersey, 1983.

33. I. Babuska and W. C. Rheinboldt, ''Error estimates for adaptive finite element computations,'' *SIAM J. Num. Anal.* **15,** 736 (1978).

34. J. M. Melenk, ''On Generalized Finite Element Methods,'' Ph. D. thesis, The University of Maryland, 1995.

.